EXPERIMENTAL SHOCK CHEMISTRY OF AQUEOUS AMINO ACID SOLUTIONS AND THE COMETARY DELIVERY OF PREBIOTIC COMPOUNDS

JENNIFER G. BLANK[1*], GREGORY H. MILLER[2], MICHAEL J. AHRENS[3] and RANDALL E. WINANS[3]

[1] *Department of Earth and Planetary Science, University of California, 301 McCone Hall, Berkeley, California 94720-4767, U.S.A.*

[2] *Applied Numerical Algorithms Group, Lawrence Berkeley National Laboratory, MS 50A-1148, 1 Cyclotron Rd, Berkeley, California 94720, U.S.A.*

[3] *Chemistry Division, Argonne National Laboratory, 9700 S. Cass Ave, Argonne, Illinois 60439, U.S.A.*

([*] Author for correspondence, e-mail: jenblank@seismo.berkeley.edu)

(Received 10 November, 1999)

Abstract. A series of shock experiments were conducted to assess the feasibility of the delivery of organic compounds to the Earth via cometary impacts. Aqueous solutions containing near-saturation levels of amino acids (lysine, norvaline, aminobutyric acid, proline, and phenylalanine) were sealed inside stainless steel capsules and shocked by ballistic impact with a steel projectile plate accelerated along a 12-m-long gun barrel to velocities of 0.5–1.9 km sec^{-1}. Pressure-temperature-time histories of the shocked fluids were calculated using 1D hydrodynamical simulations. Maximum conditions experienced by the solutions lasted 0.85–2.7 μs and ranged from 5.1–21 GPa and 412–870 K. Recovered sample capsules were milled open and liquid was extracted. Samples were analyzed using high performance liquid chromatography (HPLC) and mass spectrometry (MS). In all experiments, a large fraction of the amino acids survived. We observed differences in kinetic behavior and the degree of survivability among the amino acids. Aminobutyric acid appeared to be the least reactive, and phenylalanine appeared to be the most reactive of the amino acids. The impact process resulted in the formation of peptide bonds; new compounds included amino acid dimers and cyclic diketopiperazines. In our experiments, and in certain naturally occurring impacts, pressure has a greater influence than temperature in determining reaction pathways. Our results support the hypothesis that significant concentrations of organic material could survive a natural impact process.

Keywords: amino acids, comets, impact delivery, origin of life, shock recovery experiments

1. Introduction

The Earth was formed by the gradual accretion of planetesimals, bodies resembling meteorites and comets, which were likely to have been rich in organic compounds. Complex organic molecules from these extraterrestrial sources have been widely discounted in the organic carbon budget of the prebiotic Earth because they were considered likely to have been destroyed by the heat liberated during impact (Chyba *et al*., 1990; Chyba and Sagan, 1997; Thomas and Brookshaw, 1997). While some researchers have suggested that organic molecules could be delivered

Origins of Life and Evolution of the Biosphere **31:** 15–51, 2001.

to the Earth intact (Oró, 1961; Clark, 1988; Blank and Miller, 1998; Pierazzo and Chyba, 1999), their arguments have not been tested previously in the laboratory.

The majority of organic carbon in the pre-biotic Earth is believed to have been produced from the interaction of simple gases and ultraviolet light, lightning, and coronal discharge (Miller and Urey, 1959; Chyba and Sagan, 1992, 1997), and through processes occurring in submarine hydrothermal vents (Russell *et al*., 1988; Shock, 1990). Most of the organic compounds from exogenous sources, perhaps as much as 15% of the total organic carbon on the Earth (Chyba and Sagan, 1997), originated from a steady rain of interplanetary dust particles reaching the surface of the planet without experiencing catastrophic impact. Organic carbon compounds derived from meteors and comets are considered to be of terrestrial origin. This is because of a consensus that pre-existing organic compounds would completely dissociate (pyrolize) in the impact process but may participate in the formation of new organic materials in the terrestrial environment (Barak and Bar-Nun, 1975; McKay and Borucki, 1997).

Comets are composed of water ice, silicates, metal oxides and sulfides, and a collection of simple and complex organic molecules comprising as much as 15 wt % of the total cometary body (e.g., Fomenkova *et al*., 1994). Such chemistry is favorable for the evolution of complex organic molecules. Oró (1961) remarked on the probable composition of comets, then known from remote spectroscopic observations, and proposed comets as a significant source of organic molecules during the early history of the Earth and possibly for prebiotic synthesis that led to the development of life. Carbon-rich particles sampled in comet Halley's coma (Kissel *et al*., 1986; Kissel and Krueger, 1987) appear to contain complex organic compounds, including unsaturated linear and cyclic molecules which may have prebiotic significance (Huebner and Boice, 1992). Lerner *et al*. (1993) observed that an aqueous solution of a model cometary composition combined with mineral grains from a chondritic meteorite produced amino acids via a Strecker-type mechanism, through reaction of an aldehyde with ammonium and HCN. This may be the origin of abundant amino acids discovered in chondritic meteorites (Cronin and Chang, 1993). Whether this reaction occurred on Earth, and whether it contributed to the development of terrestrial life, is a subject of active debate (e.g., Greenberg, 1993).

The flux of organic matter to the Earth via comets and asteroids, averaged over the period of heavy bombardment prior to 3.8 Gyr, may have been as high as 10^{13} kg yr^{-1} (calculated from data in Chyba *et al*., 1990; see also Zahnle and Sleep, 1997). This estimate is substantially larger than the value of (5×10^{8}) to (5×10^{12}) kg yr^{-1} estimated to originate from the terrestrial environment (Chyba and Sagan, 1997). Even a small fraction of this material, delivered in a cometary body, could have a significant influence on the global budget. In addition, impact delivery may potentially localize this flux in space and time, leading naturally to concentrations of organic material significantly above levels easily achieved by endogenous production mechanisms.

The principal argument against direct delivery of organic material to the Earth focuses on the very high temperatures expected in a high-velocity impact. Any impactor must have a minimum relative velocity of 11.2 km s^{-1} (the escape velocity for the Earth), and this value helps to constrain the possible temperature ranges a comet might experience. Chyba and others (1990) calculated maximum peak temperatures of 40 000 K would be reached if all the kinetic energy of an 18 km s^{-1} comet were converted to heat. They pointed out that this temperature, multiplied by Boltzmann's constant, is much higher than the activation energies typical for pyrolysis reactions of organic compounds (i.e., $k_B T >> E_a$) and that the resulting collision should induce complete breakdown of any organic molecules present. Subsequent modeling (Blank and Miller, 1998; Pierazzo and Chyba, 1999) suggests that special conditions such as oblique impacts may generate lower peak temperatures. Nevertheless, when temperature alone is taken as a measure of chemical stability, the possible impact delivery flux would appear insignificant in comparison to terrestrial production.

We (Blank and Miller, 1998) recently reevaluated this kinetic argument using canonical activation volumes for bond breaking (Asano and Le Noble, 1978; see also Matsumoto and Acheson, 1991). The activation volumes for bond breaking are positive, and therefore high pressures should retard the kinetics of reactions that involve the breaking of bonds (e.g., pyrolysis). We showed that at 7000 K and 100 GPa (conditions we estimated to correspond to a planar impact of a water ice comet against basaltic crust at escape velocity), the estimated rate of pyrolysis should be the same as at 900 K and 1 atm. Given the short time scale of an impact event, organic compounds present in comets might survive brief exposure to high temperature and simultaneous high pressure, and their flux to the surface of the planet could be significant. The important point we made is that peak temperature conditions occur in conjunction with peak pressure conditions. Intuition based on observations of material behavior at ambient pressure and high temperatures may be misleading.

A thermodynamic (vs. kinetic) argument can also be made for the stability of organic compounds in impacts. The Clapeyron slope for pyrolysis reactions (e.g., 110 K GPa^{-1} for the breakdown of pyruvic acid (Blank *et al*., 1997)) may be steeper than the slope of the shock Hugoniot curve (85 K GPa^{-1} for shocked ice (Blank and Miller, 1998)). This means that the thermodynamic trajectory of the shock Hugoniot, or loci of states achieved by a shocked material, tends to favor the stability of reactants versus that of pyrolysis products, in accordance with Le Chatelier's principle. This argument also favors the combination of organic monomers to form polymers, including the combination of amino acids to form polypeptides.

Organic carbon in comets might also survive if the impact velocity were sufficiently reduced by atmospheric drag. Chyba *et al*. (1990) demonstrated by numerical simulation that the impact temperatures in an atmospherically-decelerated comet could be low, <1800 K. Conditions under which aerobraking applies may

be rare, however, since small comets would fragment explosively (Hills and Goda, 1993), and large ones would not be slowed at all (Chyba and Sagan, 1997).

Even at escape velocity the temperatures incurred in oblique collisions can be slight. Shock temperatures scale with the normal component of the impact velocity, and this can be made arbitrarily small as the impact vector approaches the horizontal (Blank and Miller, 1998, Figures 1–3 therein). In this case, however, the kinetic energy of the tangential velocity component must be dissipated as heat. If that heat were distributed uniformly in the debris from the impactor, then temperatures circa 40 000 K might still occur. However, hydrodynamic phenomena (e.g., jetting; Miller, 1997, 1998) may distribute this energy heterogeneously. In fact, for some combinations of impact velocity and impact angle, parts of the outflow jet may experience very low peak temperatures (owing to the obliquity of the impact) and very low residual horizontal velocity (owing to the speed and orientation of the outflow jets). In effect, it might be possible to 'soft land' part of a comet. Clark (1988) described other possible soft landing mechanisms and pointed out that the result, a 'comet pond', would be a localized reservoir of exogenous organic matter at elevated concentration levels in aqueous solution. A specific dynamical mechanism is thereby provided for Oró's (1961) hypothesis that cometary matter might directly facilitate the origin of life.

Although the fraction of a given object that can be soft landed may be small (because the outflow jets represent a small fraction of the total impactor mass), it may be a small fraction of an arbitrarily large impactor. Since a thick atmosphere is not required, this mechanism might be operative on other terrestrial bodies (Clark, 1987). The probability of delivering a significant amount of material by the oblique impact mechanism described above is certainly small, particularly considering that the mean encounter velocity of short period comets with the Earth is not zero (as supposed by assuming the escape velocity), but distributed about a median value of $\approx$29 km s^{-1} (Chyba *et al.*, 1990; see also Steel, 1992). Very low encounter velocities ($\sim$0 km s^{-1} at ∞) are not impossible, merely improbable (cf., Clark, 1988). The oblique impact delivery mechanism can operate at larger encounter velocities, but it then requires some component of aerobraking.

Dynamical considerations (Clark, 1988; Chyba *et al.*, 1990; Blank and Miller, 1998) thus allow for the possibility of organic carbon delivery in large impacts (vs. only by interplanetary dust particles). Preliminary thermodynamic and chemical kinetics arguments support this same conclusion. It is important to recognize, however, that parameters such as the activation energy and activation volume are themselves functions of temperature and pressure, and that reaction pathways under extreme conditions may be different than those under typical laboratory conditions (Davis and Brower, 1996). The chemistry occurring in a shock process may be different than would occur under static pressure-temperature conditions even on comparable time scales (Dodson and Graham, 1982), particularly in solid-phase reactions. To be able to predict the chemistry occurring in a natural impact it is

therefore essential to obtain kinetic parameters in laboratory impact experiments under comparable conditions.

In this report, we describe new experimental and analytical techniques applied to the liquid recovery of samples that have experienced a ballistic impact. We describe our experiments below, then discuss our preliminary findings. These include the observation of that all our amino acids survived, to some extent, impact conditions in the pressure range of 5–21 GPa. We find evidence for the combination of amino acids to form dimers, possibly via peptide bonds. This is consistent with our earlier prediction (Blank and Miller, 1998) that pressure would suppress breakdown reactions such as pyrolysis and decarboxylation. This study supports the hypothesis that comets might be a source of organic matter to the Earth that may have influenced or facilitated the origin of life.

2. Related Experimental Studies

While the experiments reported here are the first to address the survival of organic material in an aqueous medium during a ballistic impact, there have been a few preliminary impact studies on the shock chemistry of the organic materials associated with carbonaceous meteorites. Tingle *et al*. (1992) reported results from three shock experiments on cored pieces of the Murchison meteorite encapsulated in stainless steel capsules. The samples experienced peak pressures as high as 19, 20, and 36 GPa, respectively, through a sequence of shock reverberations (e.g., Gibbons and Ahrens, 1971). Recovered samples were analyzed by thermal desorption photoionization mass spectrometry, and the authors noted little change in the organic constituents of samples shocked to peak pressures $\leq$20 GPa. However, approximately 70% of the original organic matter was lost from the sample exposed to a 36 GPa impact, and the residual organic compounds appeared to have a lower C/H ratio than the starting material, suggesting that the bulk composition had changed. As neither peak temperatures nor time-temperature-pressure histories of the samples are reported, the connection to chemical thermodynamics and kinetics cannot be made. Nonetheless, it is significant that organic material survived the extreme conditions of an impact to some degree. Peterson and others (1997) conducted a series of similar shock experiments over a pressure range of 3.5–32 GPa using powdered Murchison and Allende meteorite samples stripped of their original organic carbon and subsequently doped with well-characterized amino acids whose breakdown and reaction products were readily measured and distinguished. In these experiments, the abundance of residual amino acids was found to diminish substantially with high pressures, with typically 50% loss by 30 GPa. The formation of new daughter amino acids was inferred, in particular the decarboxylation of aspartic acid to form β-alanine. The porosity of the powdered starting material was not reported for these experiments, and shock temperatures are very sensitive to porosity. Porous materials experience substantially higher tem-

perature for a given shock pressure than do solids of the same material (Kieffer, 1971). The T(P) conditions of the Peterson *et al*. (1997) experiments are likely very different from the T(P) conditions of the Tingle *et al*. (1992) experiments. In summary, neither Tingle *et al*. (1992) nor Peterson *et al*. (1997) focused on the temperature of their experiments. Instead, they discuss the breakdown of organic materials in terms of degree of shock loading.

Shock wave techniques to measure rates of chemical reaction have been applied extensively to the study of organic gases (e.g., Wu *et al*., 1987; Mertens *et al*., 1989; Mackie *et al*., 1990; Hidaka *et al*., 1993; and Davidson *et al*., 1993). However, chemical reaction pathways occurring in shocked gases, and their measured rates, are likely to be significantly different than in shocked organic liquids and solids because of the very different P,T conditions obtained. Shocked gases have significantly higher temperatures than shocked liquids or solids for a given shock pressure. (For example, an ideal gas shocked to 10 GPa will reach a temperature that is on the order of six thousand times higher than that of ice shocked to the same pressure). The occurrence of shock-induced chemistry in organic liquids and solids is well-documented (e.g., Dodson and Graham, 1982; Dremin and Babare, 1982; Davis and Brower, 1996), but corresponding parameters have not been determined.

3. Choice of Starting Materials

Comets consist of a mixture of ices (H_2O, CO_2, NH_3, HCN, etc.) and rock, in varying (and uncertain) proportions, though the ice component is dominantly water. We used water as our analog for a cometary matrix and prepared aqueous starting solutions containing dissolved amino acids.

Since amino acids were first identified (e.g., Degens and Bajor, 1962; Kvenvolden *et al*., 1970) as compounds indigenous to extraterrestrial samples (cf., Cronin and Chang, 1993), their presence and high abundance in carbonaceous chondrites has been of considerable interest. To date, more than 70 amino acids have been identified in meteoritic samples (Cronin and Pizzarello, 1986; cf. Cronin and Chang, 1993). An important question concerning their origin is whether they formed in the chondrite parent body or originated in the interstellar medium. Cronin and Pizzarello (1986) hypothesized that the amino acids formed in Murchison meteorite via Strecker synthesis. In the latter case they would be expected to exist in comets, although cometary amino acids have not yet been detected (cf., Snyder, 1997).

We chose amino acids having a high solubility in water, in order to facilitate detection, and a variety of functional groups, in order to maximize possible differences in response to the impact process. LD-2-aminobutyric acid (Amb) and L-norvaline (Nor) are uncommon in laboratory environments and have been identified in the Murcheson meteorite (Kvenvolden *et al*., 1970). L-lysine (Lys) and L-phenylalanine (Phe), are among the most common amino acids, while D-proline (Pro) is somewhat rare. Lysine, the amino acid with the strongest base character,

contains two amine functional groups. Phenylalanine is an aromatic compound and proline incorporates its amine group within a 5-membered ring.

In later experiments, we added adamantanone ($C_{10}H_{14}O$) to the starting solutions. We expected that adamantanone, with its diamond-like structure, would be resistant to break down and could serve as a tracer. As we observed no trace of adamantanone or clearly related derivatives in the shocked liquids originally carrying it, we reverted to solutions containing amino acids only.

Standard solutions used in our experiments were characterized by high performance liquid chromatography and mass spectrometry, described below. We obtained the amino acids from Aldrich Chemical Co. (Milwaukee, WI, U.S.A.) and did not purify them further before use. Solvents (methanol, methylene chloride, acetone, and water) used in this study were of high purity (HPLC-grade) and purchased from Fisher Scientific (Fairlawn, NJ).

4. Experimental Method

4.1. Experiment objectives

The goal of our laboratory experiments was to shock aqueous solutions and recover them for chemical analysis. Experiments were conducted using a laboratory gun to fire a 304L stainless steel projectile at a steel capsule housing a liquid sample. Because a sample contains less than a milligram of organic matter and each firing of the gun generates a few kilograms of organic soot, it is essential that the sample capsule remain intact throughout the shock and recovery process. Otherwise, ambient contamination may overprint the signal of any of the organic chemistry associated with the shocked fluids.

We also wish to subject a sample to conditions that may be characterized accurately in terms of temperature and pressure histories. This poses two constraints. First, it is desirable to achieve uniaxial (i.e., one-dimensional) shock pressurization or 'loading' as well as uniaxial release to room pressure ('unloading'), to the maximum extent possible. Second, the recovery process should be 'gentle' so as to avoid subjecting the sample capsule to secondary shocks, not to mention to increase the likelihood of sample recovery. Meeting both of these constraints serves to simplify the history of a sample and improves our ability to predict its history through numerical modeling.

Our experimental approach was adapted from methods used by Dr. George Gray (Los Alamos National Laboratory) to shock and recover engineering materials (Gray, 1993). Similar approaches have been described by Orava and Whittman (1971) and Decarli and Meyers (1981). As mentioned above, the strategy is to follow design rules that result in *uniaxial* loading and unloading of the sample, provided it has the same shock impedance as the capsule. Shock impedence is the product of density (ρ) and shock velocity (U_s); ρU_s. It is the generalization

of accoustic impedence (ρc), where c is the speed of sound. Sound waves do not reflect off a material interface when the accoustic impedences are the same on both sides of the interface. Likewise, if there are no shock impedence discontinuities within the capsule, then rarefaction waves will be created only at the free surface of the capsule. When rarefactions originating at different points intersect within the capsule, the capsule experiences tension, and may crack or otherwise fail. The design rules we followed guaranteed that such failures occurred only in the 'expendable' regions way from the sample capsule. Furthermore, the cracks generated in these expendable regions could not propagate across surfaces interior to the capsule, and the fluid-filled capsule was protected from rupture.

Following our design strategy, the resulting sample volume was a cylinder with an aspect ratio of approximately 31:1 (diameter vs. thickness). Given the dimensions of our gun barrel with its 80-mm inner diameter, the volume diameter was constrained to be $\sim$12.7 mm in order that edge effects (rarefactions originating at the projectile circumference) did not disturb the liquid sample. This, and our 31:1 aspect ratio, allowed a maximum volume of $\approx$50 μL. We assume that if the shocked fluid in the sample volume has experienced loading and unloading uniaxially to a rigorous degree, its time-temperature-pressure history is independent of its radial location and can be computed with standard 1-dimensional methods.

4.2. Capsule design and preparation

As mentioned in the preceding section, the dimensions of the gun and our adherence to strict design strategies resulted in a very small volume of fluid per experiment. Consequently, capsule preparation required careful, high-precision machining. Both the target assembly and the projectile flyer plate were machined from 304L stainless steel. This material has a low tendency to work harden and under room conditions is not reactive with the aqueous sample solution.

The sample capsule (Figure 1) was first machined as two separate components, with an approximately 0.001′ (0.0254 mm) interference fit on the boss. Prior to joining the two sample capsule components, the interior surfaces, the 0.010′-diameter (0.254 mm) sample fill hole, and the 0–80 (English tap) threaded closure, were finished. This first machining step was completed using standard machining oils and tapping fluids. After machining, the parts were cleaned carefully to remove any organic residue. The male and female components of the sample assembly were cleaned together with 0–80 set screws using a 4-step procedure. The parts were washed first in methylene chloride ultrasonically for 10–15 min. The solvent was decanted, then the wash was repeated. Next, the parts were washed ultrasonically for 10–15 min with acetone, methanol, then twice with water. All solvents were HPLC (high-performance liquid chromatography) grade. The parts were dried for 1–2 hr at 120 °C, then cooled to room temperature. After the cleaning, a 0–80 set screw was placed in the tapped closure hole to protect the fill hole and sample capsule interior from contamination during subsequent machining steps. Even with

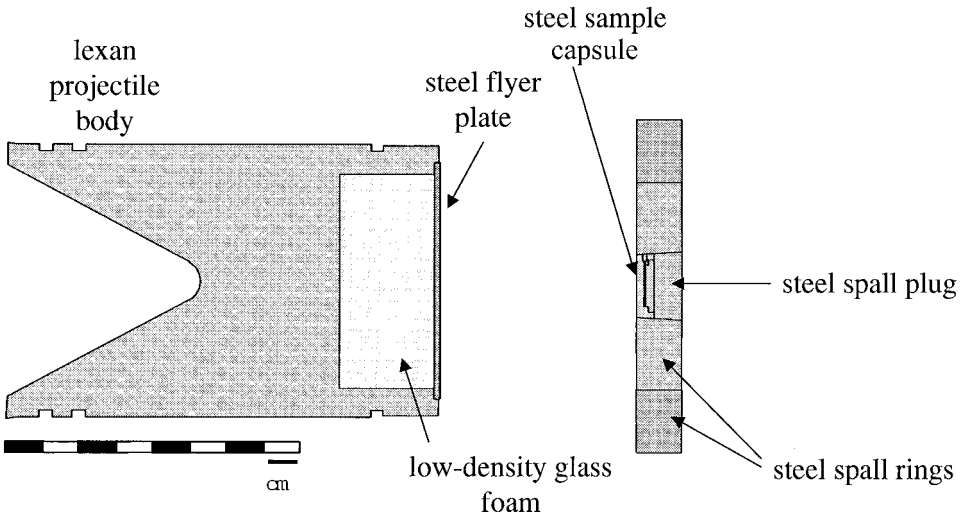

Figure 1. Schematic of projectile and target assemblies. The lexan projectile body is loaded into the front end of the barrel and propelled down the length of the gun. The steel flyer plate impacts a stationary target, consisting of the capsule and associated spall plug and rings. Steel components are machined from 303L stainless. The samples are contained in a wafer-shaped volume ($\approx$50 μL) in the interior of the capsule.

this precaution, the final machining steps were carried out without machining oils or cutting fluids.

The second machining phase involved heating the female component of the sample capsule on a hot plate to facilitate fitting of the male and female components. Once fit, the only access to the sample capsule was through the fill hole, which was kept closed with the set screw. The male and female components were then electron beam welded along the circumference of the boss, and to the full depth of the shoulder. After welding, the outside surfaces of the sample capsule were machined without any oils or cutting fluids.

After final machining, the sample capsule was weighed and its interior volume determined by repeated filling and extraction of HPLC grade methanol. Filling was accomplished using a micro-syringe with a 10 μm-diameter silica needle. Methanol was found to give reproducible volume measurements consistent with the design sample volume of $\approx$50 μL. Other solvents including water tended to give low volume measurements, presumably due to the presence of air bubbles trapped inside the capsule. The methanol was removed using the micro-syringe and the sample was dried at 120 °C, cooled to room temperature, then filled with the sample solution. A small piece of gold wire (cleaned with the same 4-step process as the sample capsule components) was placed at the bottom of the 0–80 tapped hole, and then the capsule was sealed with a 0–80 steel socket head cap screw. Tightening the screw deformed the gold wire, eliminating void space from

the filled capsule assembly and sealing the capsule. The protruding portion of the socket head screw was removed by hand filing without lubricants.

The filled sample capsule and its matching spall plug (Figure 1) were press fit into the spall ring assembly by hand, and seated with a light hammer blow to the back surface of the spall plug. The details of this final assembly step are critical, as any void space, especially between the spall plug and sample capsule, will lead to shock wave interactions that may cause the sample capsule to fail. To promote a tight, void-free fit, the circumference of the sample capsule and spall plug, and the interior surface of the spall ring, were carefully hand lapped. The surfaces were coated lightly with molybdenum disulfide lubricant to fill any irregularities in the surface caused by scratches. This completed the construction of our sample assemblies in our first series of experiments. In later series, we attached a thin ($\approx$1.8 mm) cover plate in front of the target assembly. The purpose of this extra plate was to provide a buffer between the sample capsule and flyer plate, to protect the sample capsule from possible shear motion that would interfere with its separation from the spall ring after impact. The buffer plate was attached with four screws located near its circumference, outside the diameter of the flyer plate.

4.3. SHOCKWAVE EXPERIMENT

The assembled target was suspended from a 6.35 $\times$ 19.05 mm aluminum bar, which was attached with screws to the outside circumference of the outer spall ring using a steel L bracket. The assembly was aligned with the gun barrel using a laser projected from the breech (Figure 2). The downrange free surface of the suspended sample assembly was $\approx$1.3 mm from the up-range end of a steel 'anvil', a 23-cm-long obstacle, whose purpose was to prevent the spall ring, projectile fragments, and other debris from following the shocked capsule into the recovery tank. The capsule, and pieces of the spall plug behind it, traveled through a 2.5 cm hole in the anvil, continue through a 1-m-long pipe, and entered a recovery tank filled with wet and dry felt. This medium served to bring the capsule to a relatively gentle stop.

Following alignment, the gun, impact tank, and catch tank were isolated and their volumes are evacuated for several hours until attaining pressures of 50–200 millitorr. A solenoid-driven pin initiated the burning of 200–2000 g of smokeless powder, accelerating the projectile down the barrel. We nominally used 22.5 g of SR7625 smokeless powder as a primer, contained in a 50 caliber primed cartridge. In high-velocity experiments, the remaining propellant consisted of IMR7828. The IMR7828 is relatively slow burning and does not burn to completion if used alone in amounts less than about 1500 g. To promote complete combustion in lower speed experiments, we used mixtures of IMR7828 and Hercules Bullseye or IMR3031. These powders differ in grain size, with Bullseye < SR7625 < IMR3031 < IMR7828, and the correlation between their proportions and the resulting projectile velocity is empirical.

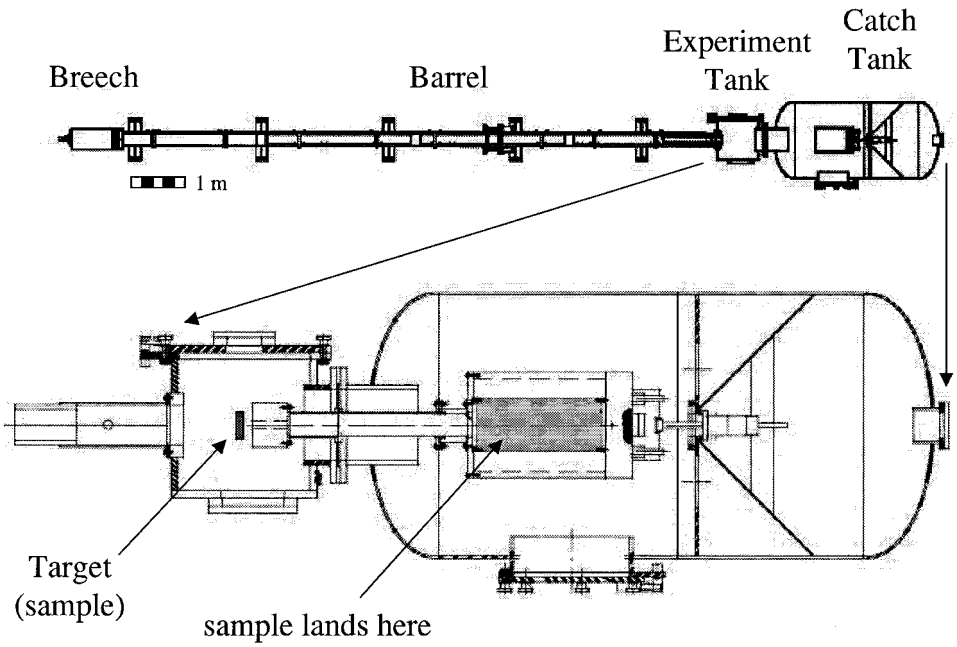

Figure 2. (a) Gun schematic. Projectiles loaded in to the breech along with gunpowder are accelerated along a barrel 12 m-long with an 80 mm-inside diameter to reach final velocities in the nominal range of 0.5–2.5 km s^{-1}. Impact occurs in the first chamber (experiment tank) and debris is collected in the second chamber (catch tank); both are shown in (b) as they are configured for shock recovery experiments. Inside the catch tank is a sample recovery tank that is filled with wet and dry wool felt to gently decelerate the shocked sample chamber. Extending from this recovery tank into the catch tank is a hollow pipe that ends in a 25.4 cm diameter steel anvil with a 2.5 cm diameter through-hole. This anvil stops the spall ring, flyer plate, and other energetic material so that it can not follow the shocked sample chamber into the recovery tank. Not shown are two 2.54 cm thick expendable steel plates and four 1.9 cm-thick expendable plywood plates that are attached to the anvil with nylon threaded rod. These extra plates, which have 2.54 cm through-holes aligned with that of the anvil, protect the anvil from damage during the experiment.

The projectile velocity was measured in the barrel near the experiment tank using four pairs of electrical shorting devices, each pair separated by 100.0 mm. The stations consisted of signal wires (made of #77 drill blanks) and grounding tabs (made of Cu foil). Electrical contact was made between the signal wire and its grounding tab when the steel flyer plate of the projectile impacts the wire. The time intervals between these shorting events determined the projectile velocity. No other measurement was made during the impact event. Changing the mixture and total mass of gunpowder loaded into the breech varied the projectile velocities. Increasing the thickness of the metal flyer plate lengthened the duration of the shock pulse experienced by the sample. Flyer plate thickness ranged from 2.0–4.0 mm, corresponding approximately to a factor of 3 variation in shock pulse interval.

Upon impact with the flyer plate, the sample assembly separated violently. The spall plug (usually fractured in two pieces) and the sample capsule flew through the hole in the steel anvil. Other debris, including the remnants of the projectile and spall rings, did not pass through this throat but were diverted sideways. Downrange of this debris-stripping assembly, the sample capsule and spall plug fragments came to rest in the recovery chamber, situated in the catch tank (Figure 2).

Immediately following an impact experiment, the tanks were returned to room pressure while ventilated using an exhaust fan. The door of the catch tank was opened, and one of us (GHM) entered the tank to release the recovery chamber from the debris-stripping anvil. The inner barrel of the catch tank was then pivoted 90°, perpendicular to the gun barrel, to allow access to the felt packing. The pads of felt were examined individually until the sample capsule was located. The sample capsule was inspected, cleaned with methanol-soaked towels to remove soot, wool fragments, or other debris, and then placed in a clean Teflon container. The sealed Teflon container was stored in a refrigerator prior to analysis.

Conditions of our experiments are summarized in Table II.

4.4. LIQUID RECOVERY

Extraction of the shocked fluid required opening the sample capsule by milling perpendicular to the fill hole. Milling was performed without solvents or oils. The sample capsule was not heated noticeably, and the capsule remained below room temperature during the entire procedure. Typically, we observed the gold wire that had been used to seal the capsule and were able to either extract it with a final pass using the mill or pluck it out using metal tweezers cleaned with dichloromethane. Once the gold was removed, the liquid well was exposed, and a syringe was inserted in order to extract residual liquid. When fluid extraction was not possible by this technique, measured aliquots of HPLC-grade water were injected into the capsule with a syringe, then withdrawn, measured again and collected. We interpreted the extraction difficulties to indicate that the amount of fluid remaining in the capsule was too small (presumably due to leakage after the shocked capsule was recovered from the gun), or that ductile deformation of the capsule prevented our access to the fluid reservoir using a syringe.

Note that our recovery procedure precluded capture of any volatile components associated with the fluid under ambient conditions. The recovery procedure described here was successful in that our fluid samples were subjected to well-characterized shock conditions, and some fluid was recovered, all without detection of any contaminants. To date, we have so far been unable to achieve complete quantitative recovery of the fluid, however, which complicates our interpretation of chemical kinetics.

We experienced three principal experimental difficulties. In some experiments, the sample capsule was split apart completely whereas the spall plug was recovered intact. This type of failure was most likely the consequence of the presence of a

TABLE I
Composition of initial aqueous solutions

Amino acids			Standard solution									
Abbreviation		MW	A		B		C		C′[a]		D	
		(g mol^{-1})	Molality	g mL^{-1}	Molality	g mL^{-1}	Molality	g mL^{-1}	Molality	g mL^{-1}	Molality	g mL^{-1}
L-lysine	Lys	146.19	0.5440	0.0795	0.5310	0.0776	0.1008	0.0147	0.1008	0.0147	0.1004	0.0147
L-norvaline	Nor	117.14	0.3780	0.0443	0.3580	0.0419	0.0714	0.0084	0.0714	0.0084	0.0770	0.0090
DL-2-aminobutyric acid	Amb	103.12					0.1021	0.0105	0.1021	0.0105	0.0958	0.0099
L-phenylalanine	Phe	165.19					0.0920	0.0152	0.0920	0.0152	0.0901	0.0149
D-proline	Pro	115.13					0.0714	0.0082	0.0714	0.0082	0.0753	0.0087

[a] Solution ‘C′ ’ was made by adding 2-adamantanone (MW 150.22) to an aliquot of Solution C at near saturation level (≈0.0067 mol L^{-1}).

small gap between the spall plug and the sample capsule. Spall and catastrophic sample loss could result from rarefactions from the back of the flyer plate and the downrange end of the sample capsule colliding within the sample capsule. More commonly, the sample capsule was recovered intact, but several hours later a bead of fluid could be observed weeping from the vicinity of the fill hole, or from the center of the up-range face of the sample capsule. Leakage around the fill hole could be due to plastic deformation of the capsule assembly, and we introduced the sample cover plate to reduce this deformation. Leakage from the center of the up-range face of the capsule could result from the fluid-steel impedance mismatch. Two-dimensional numerical computations of these impacts suggest that a rarefaction in the steel, originating at the fluid-steel interface, place the center of the sample capsule in tension. A consequence of this tension may be microscopic fractures through which fluid may leak. In future experiments, we intend to try aluminum as the target material (the water-aluminum impedance mismatch is significantly smaller than that for water-steel). Finally, in one experiment the shocked sample capsule was not found in the wet felt, but was instead found inside the experiment tank. In this case the capsule was hot to the touch, and some chemistry was probably induced by this high temperature but low pressure condition. This failure mode was attributed to deformation of the spall ring preventing the clean separation of the shocked sample capsule. The addition of cover plates prevented this failure mode.

5. Analysis

5.1. Hydrodynamical modeling of impact histories

The time-temperature-pressure records of shocked fluid samples were calculated using numerical integration of one-dimensional Euler equations for inviscid, compressible flow applied to our design geometries. We ignored thermal conductivity, as the timescales of thermal diffusion are long relative to the $\sim\mu$s duration of an experiment's shock pulse. Our numerical resolution was approximately 0.4 microns, resulting in 100 cells across the fluid volume. Such high resolution was essential to minimize temperature errors arising at the fluid-capsule interface and precludes reasonable 2- and 3-dimensional modeling at this time. Our one-dimensional calculations were based on an algorithm described by Miller and Puckett (1996), modified to accommodate the equations of state needed here. We used a Mie-Grüneisen equation of state, which describes the change in pressure with energy at a constant specific volume, to model the 304L stainless steel. Parameters for steel are tabulated in Marsh (1980). We used a Bakanova formalism to describe the equation of state of the aqueous solution by extrapolation to different energy states along paths of constant pressure. Details of our model for the fluid are given in Blank and Miller (1998).

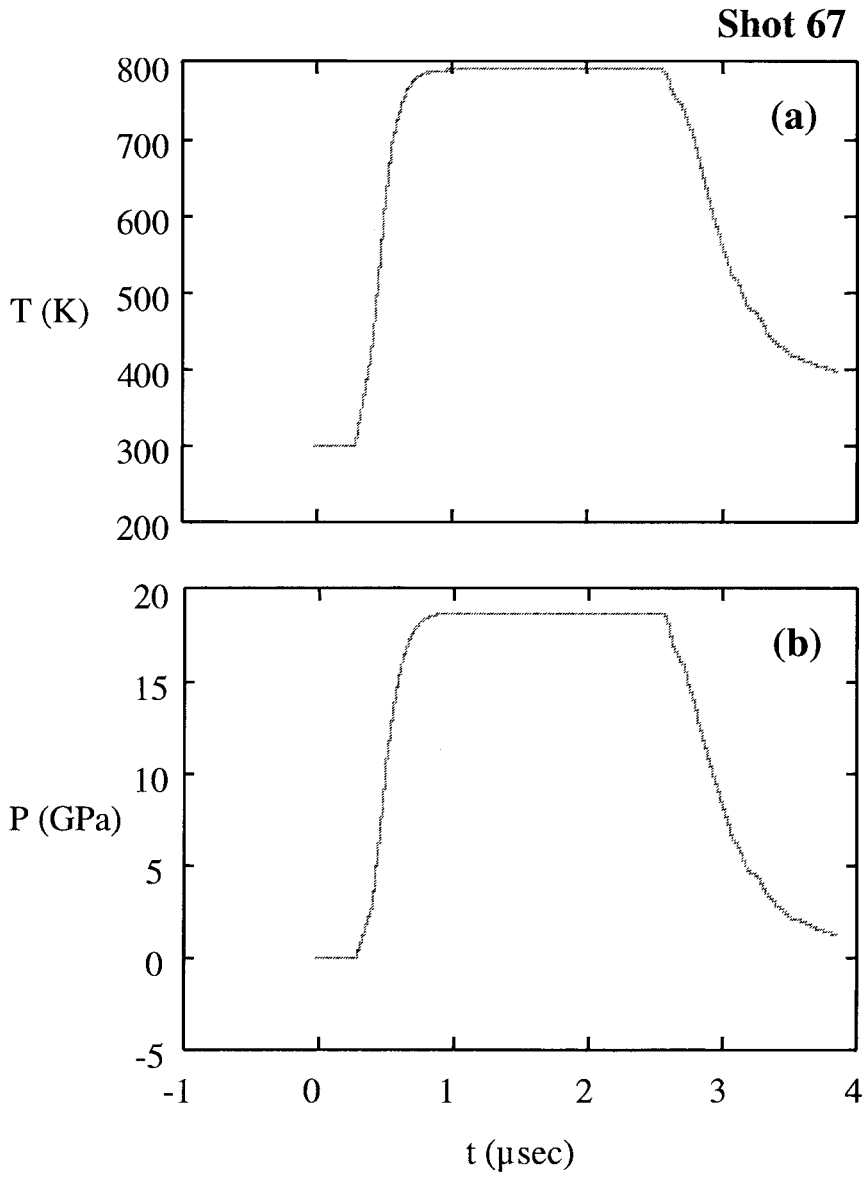

Figure 3. Volume-averaged 1D computation of (a) sample pressure history, and (b) sample temperature history, for sample #67. These profiles reach a plateau state where the pressure equals the pressure that the sample assembly would have reached if solid (without a fluid-filled sample region).

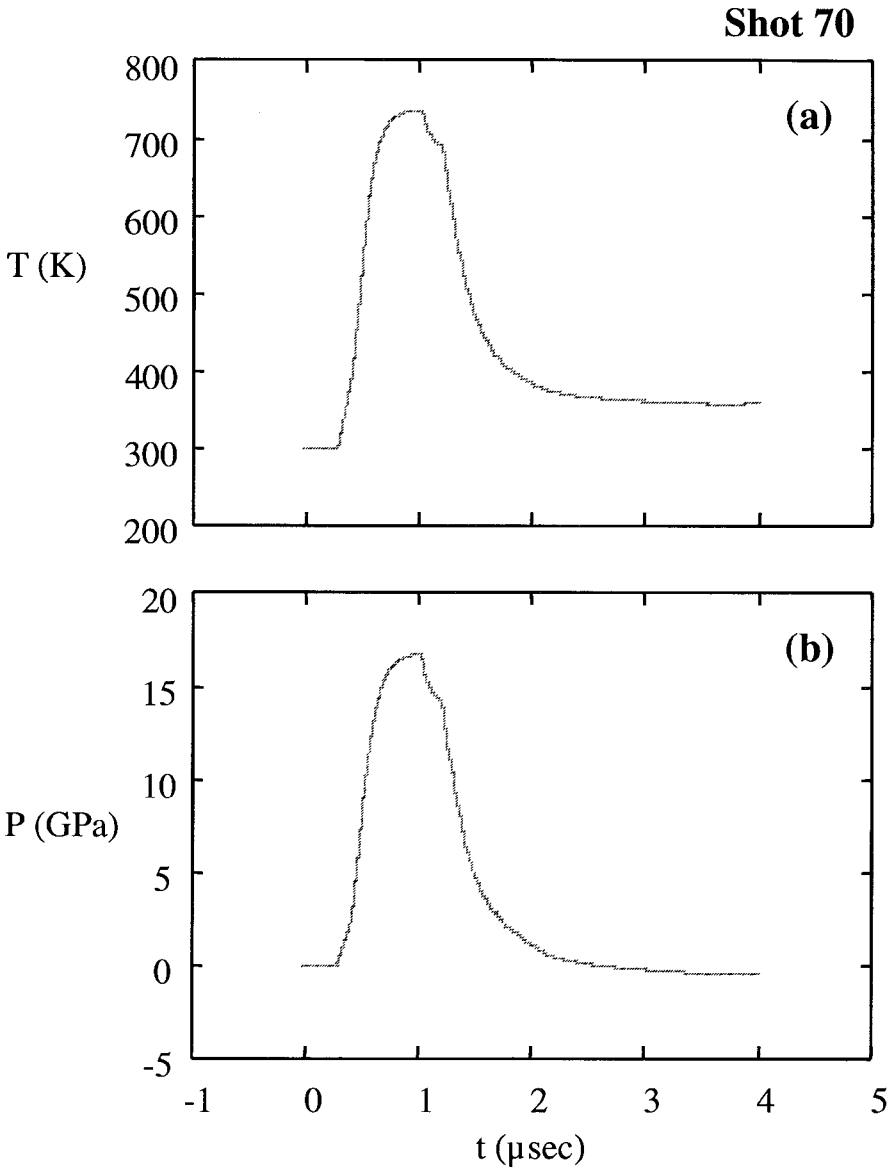

Figure 4. Volume-averaged 1D computation of (a) sample pressure history, and (b) sample temperature history, for sample #70. The pressure reaches the ideal value (that would have been obtained if the capsule were solid) to within 1%, but is released immediately, so no plateau is observed.

TABLE II

Summary of experimental conditions and calculated temperature-pressure-time histories of shocked fluids

Shot	Experiment Summary						Calculated Fluid Histories		
No.	Flyer Plate d (mm)[a]	Impact u (km s^{-1})[b]	Container P (kbar)[c]	Initial Solution[d]	Recovery Condition[e]	Liquid Recovered[f]	T_{max} (K)	P_{max} (GPa)	Time (μsec)[h]
64	1.97	0.31	58.8	A (20.2 mg)	Intact	Y	412	5.1	1.05
67	6.34	0.90	187.0	A (27.6 mg)	Intact[g]	N	740	18.5	2.70
70	2.01	0.82	167.7	B (60.1 mg)	Intact	Y	740	16.5	0.90
71	1.96	0.88	182.2	B (43.3 mg)	Intact	N	770	18.0	0.85
72	2.05	0.91	188.5	C (53.7 mg)	Intact	Y	790	19.0	0.95
73	4.00	0.89	184.8	C (46.9 mg)	Intact	Y	780	18.5	1.70
76	**2.01**	0.95	197.9	C′ (43.7 mg)	Intact	Y	810	20.0	0.95
77	**3.96**	0.95	197.5	C′ (67.7 mg)	Intact	Y	810	20.0	1.70
78	**1.99**	1.03	216.3	C′ (55.8 mg)	Intact	Y	870	21.0	0.90
91	**1.99**	0.93	190.0	D (82.4 mg)	Intact	N	880	19.5	0.90

[a] Flyer plate diameters listed in bold type indicate presence of 4 mm shims adjacent to plate during experiment.
[b] Projectile velocity was measured directly using 4 pairs of pin indicators at 100 cm intervals along the portion of the gun barrel adjacent to the experiment tank.
[c] Calculated using impact velocity and impedence match solution for collision of two stainless steel (304L) objects.
[d] Initial liquid composition (see Table 2) and amount sealed in sample container.
[e] Container appearance after an experiment.
[f] Yes/No (Y/N) indication of whether liquid was observed following recovery and opening of container. If no sample liquid was extracted (N), high-purity water was injected into capsule to recover residual sample material.
[g] Sample container was retrieved in experiment tank.
[h] Duration of shock pulse measured as the full-width-half-maximum of the peak PT conditions experienced by a container.

The results are volume-averaged thermodynamic histories of our samples. A commonly employed assumption in experiments of this general nature is that the peak pressure experienced by the sample was equal to the maximum pressure that the sample capsule would attain if it were solid, rather than filled with a different medium. We note that this assumption is valid for our longer-duration experiments; for example, the calculated sample pressure for Shot 67 (peak shock pulse = 2.7 μs) reaches a plateau equal to that of the stainless steel capsule (Figure 3). In shorter-duration experiments, such as Shot 70 (Figure 4; peak pulse = 0.8 μs), our calculated peak pressures are within 1% of the pressure value predicted more simply. Temperature histories must be calculated by the more elaborate procedure in both cases. Here, we characterized our calculated pressure-time and temperature-time profiles with three parameters (Table I): the peak pressure, the peak temperature, and the shock duration (estimated from the full width at half maximum of the temperature profile). The temperature histories of our samples are low relative to those of the shocked states of ice or water subjected to a *single* shock to a comparable pressure. This is a consequence of our sample design and the fact that the sample capsules are brought to their maximum pressure and temperature conditions through a succession of shocks as the shock waves reverberate within the fluid. This 'ringing up' (Gibbons and Ahrens, 1971) occurs because of the impedence mismatch between water and steel.

5.2. CHEMICAL ANALYSIS OF SAMPLES

Organic compounds in the starting solutions (Table I) and shocked samples were identified using a combination of high performance liquid chromatography (HPLC) and mass spectrometry (MS). Chemical analyses were determined using a Hewlett-Packard HP 1100 system equipped with a diode-array detector (DAD), an on-line degasser, a heated column compartment and an autosampler and automatic injector. The HPLC was connected directly to an atmospheric pressure chemical ionization (APCI) chamber and an ion trap in-line to a Finnigan model LCQ mass spectrometer.

Compound separations were achieved using a reversed phase, 250×4.6 mm, 5-micron Zorbax C18 column. The temperature of the column was held constant at 30 °C. The elution procedure, developed specifically for the separation of the 5 amino acids considered in this study (Ahrens *et al.*, in press), included a 36-min, 3-step solvent gradient. This consisted of five minutes of 100% 0.1 M acetic acid followed by a 1.5-min transition to 100% methanol and finally 29.5 min with 100% methanol. The flow rate through the column was held constant at 0.500 mL min^{-1}. All analyses were performed after sufficient equilibration of the column with the acetic acid mobile phase. In between sample analyses, 10 μL water blanks were injected and moved through the column to verify that the background spectrum intensity was at a minimum.

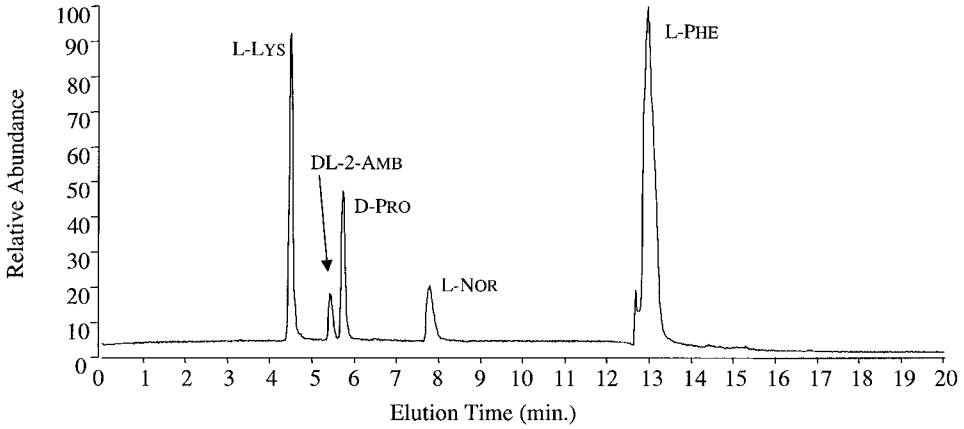

Figure 5. Representative Total Ion Chromatogram (TIC) (50–500 m/z) of a standard, illustrating the different elution times for the 5 amino acids used in the experiments (solution (Table I). A reverse-polar ion exchange column was used as the stationary phase; the gradient for the mobile phase is described in the text. Peaks correspond to: Lys (4.5 min), Amb (5.4 min), Pro (5.7 min), Nor (7.8 min), Phe (13.0 min). Peak at 12.88 min corresponds to column bleed, verified through comparison with a water blank.

Solution aliquots injected into the HPLC were typically 10 μL of sample that had been diluted by a factor of 10^2–10^3 with distilled H_2O. A representative chromatogram of a five amino acids standard in aqueous solution is shown in Figure 5.

A sample of soot collected from the recovery chamber was extracted with toluene and characterized using laser desorption mass spectrometry and high resolution mass spectrometry. Analysis revealed the presence of higher molecular weight (MW > 300) polyaromatic hydrocarbons.

5.3. CALIBRATION OF THE HPLC

In order to quantify the yields of our samples, the mass spectrometer was calibrated using standard solutions containing known concentrations of our compounds of interest. This was accomplished by dilution of a standard (typically by a factor of 100) with high-purity water, followed by consecutive analyses of the solution using the autosampler to decrease the volume of solution injected into the chromatographic column. We calibrated both 2- and 5-amino acid solutions on more than one occasion to verify that the instrument response was consistent over time (Figure 6). In general, the mass spectrometer detector exhibited a linear response to increasing concentration of the amino acids for lower concentrations. The response to Phe deviated from a straight line and was better described by a second-order polynomial, though at low concentrations ($<1.5 \times 10^{-4}$ g on column) a linear approximation agrees to within 10%.

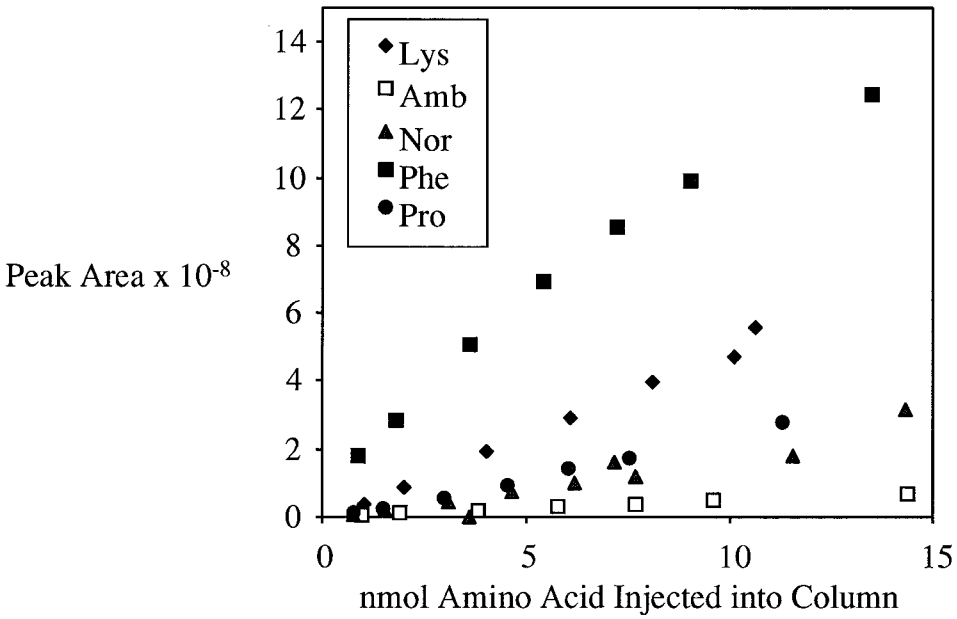

Figure 6. Calibration of the LCMS response to the 5 amino acids in this study. A series of aliquots of a known composition (Standard C), decreasing from 15 to 1 μL, was injected into the column and used to quantify the MS response. The amino acids rank in order of decreasing sensitivity to the MS detector as follows: Phe > Lys > Pro > Nor > Amb. A reproducible, linear response was observed for low concentrations (<15 nmol) of an amino acid injected into the chromatographic column, though with increasing concentrations the detector response is better described by a 2nd-order polynomial. Phe was the exception, with a smaller range (0–6 nmol) of linear response. Details of this calibration, used to determine quantitative yields for our experiments, is reported in more detail in Ahrens *et al.* (in press).

6. Results and Discussion

6.1. Relevance of laboratory shock conditions to natural impacts

Sample capsules experienced peak PT conditions for times ranging from 0.85–2.7 μs. Corresponding maximum conditions ranged from 5.1–21 GPa and 412–870 K. A summary of the calculated fluid histories of ten successful liquid recovery shock experiments is given in Table II.

We compare our laboratory conditions to a natural impact as follows: a lab pressure of 5 GPa (our minimum) corresponds to the pressure in a comet-earth (ice-serpentine) collision at a normal velocity of 1.5 km s^{-1}, according to the methods described in Blank and Miller (1998; cf., Figure 3 therein). A comet with an initial velocity of 11.2 km s^{-1} (the Earth's escape velocity) would have to impact the Earth at 7.7° from the horizontal to experience a 5 GPa impact pressure. Correspondingly,

TABLE III
Quantitative recovery yields of liquids from two shock experiments

Shot No.	Initial liquid in capsule (μL)	Liquid recovered (μL)	Relative recovery (%)	Amino acid yields (%)				
				Lys	Amb	Pro	Nor	Phe
64	10.5	10	95	40			40	
77[a]	65.1	33	51	62	72	67	62	36

[a] Values for Shot 77 were corrected for evaporative loss, i.e., yields were calculated after adding back an amount of water that would account for the discrepancy in liquid recovered. These values for the yields therefore represent lower boundaries.

our maximum pressure of 21 GPa corresponds to an impact angle of 26.5° in a collision at escape velocity.

The escape velocity is the minimum velocity possible for an Earth collision, neglecting atmospheric drag. Short period comets have a much higher average velocity of 29 km s^{-1}. A 21 GPa impact pressure at this higher velocity would result from an impact at the shallower impact angle of 10° from horizontal. How likely are these impact angles? The probability, P, of an impact at angle ϕ from horizontal, can be described by $dP = -\cos(\pi - 2\phi)d\phi$ (Shoemaker, 1962). For an impact angle of 7.7° and lower, the probability is therefore 1.8%, and the probability of an impact at angles up to 26.5° is 19.9%, or one in five. Thus, even allowing for the larger collision velocities occurring in nature, the pressure and temperature ranges achieved in our laboratory shock experiments are relevant.

The microsecond time scale of our experiments is significantly shorter than the time scale of a natural comet-Earth impact, which, for the collision of a 1-km comet with the Earth, would be on the order of 1 sec for a 10 km diameter comet (Blank and Miller, 1998). It is therefore important to assess the influence of kinetics on reaction chemistry in order to extrapolate our results to natural scenarios.

6.2. AMINO ACID SURVIVAL

Through chromatographic and mass spectrometric analysis, we verified the survival of a portion of all five amino acids introduced in our experiments. Of primary interest is the degree to which the amino acids survived the impact conditions, and whether they retained the same relative concentrations after being shocked. We address these issues in the following sub-sections.

6.2.1. *Quantitative Yields*

From among our experiments, we were able to extract liquid quantitatively from the well of two capsules, those for Shots 64 and 77. In these two experiments, a measured amount of liquid was extracted directly from a capsule, diluted with water, and analyzed. The concentration of amino acids in the solution was then calculated using the HPLC calibration for amino acids. For the capsule from Shot 64, we

TABLE IV
Amino acid yields determined by LCMS

Shot	Soln[a]	Relative Peak Areas[b]					Normalized Peak Areas[c]			
		Lys	Amb	Pro	Nor	Phe	$(Lys/Nor)_N$	$(Amb/Nor)_N$	$(Pro/Nor)_N$	$(Phe/Nor)_N$
64	A	1.00			0.44		0.51			
67	A	1.00			0.45		0.50			
Std	*A*	*1.00*			*0.32*		*0.69*			
70	B	1.00			0.91		0.28			
70		1.00			0.92		0.27			
71	B	1.00			0.46		0.54			
71		1.00			0.50		0.50			
71		1.00			0.43		0.59			
Std	*B*	*1.00*			*0.34*					
Std		*1.00*			*0.38*		*1.82**			
Std		*1.00*			*0.38*					
72	C	0.45	0.09	0.31	0.17	1.00	0.57	0.71	1.26	0.49
72		0.45	0.09	0.32	0.17	1.00	0.57	0.72	1.30	0.49
72		0.45	0.09	0.30	0.18	1.00	0.53	0.61	1.10	0.46
73	C	0.11	0.15	0.38	0.20	1.00	0.12	0.93	1.26	0.41
76	C′	0.50	0.07	0.26	0.17	1.00	0.62	0.55	1.04	0.49
76		0.14	0.04	0.06	0.05	1.00	0.60	0.91	0.84	1.65
76		0.47	0.07	0.21	0.14	1.00	0.70	0.61	0.97	0.58
77	C′	0.58	0.09	0.26	0.22	1.00	0.56	0.51	0.79	0.37
77		0.67	0.09	0.36	0.23	1.00	0.62	0.53	1.04	0.36
78	C′	0.35	0.07	0.15	0.17	1.00	0.43	0.55	0.59	0.49
78		0.23	0.06	0.12	0.10	1.00	0.51	0.75	0.85	0.86
Std	*C′*	*0.32*	*0.06*	*0.15*	*0.10*	*1.00*				
Std		*0.35*	*0.07*	*0.17*	*0.11*	*1.00*				
Std		*0.36*	*0.06*	*0.18*	*0.11*	*1.00*	*2.34*	*0.38*	*1.47*	*7.18*
Std		*0.40*	*0.06*	*0.16*	*0.11*	*1.00*				
Std		*0.35*	*0.05*	*0.14*	*0.10*	*1.00*				
91	D	0.34	0.05	0.11	0.10	1.00	0.72	0.94	0.82	1.05
91		0.21	0.03	0.05	0.06	1.00	0.76	0.87	0.61	1.83
Std	*D*	*0.44*	*0.05*	*0.16*	*0.12*	*1.00*				
Std		*0.43*	*0.05*	*0.18*	*0.12*	*1.00*				
Std		*0.46*	*0.05*	*0.18*	*0.13*	*1.00*	*2.82*	*0.36*	*1.40*	*7.03*
Std		*0.46*	*0.06*	*0.16*	*0.12*	*1.00*				
Std		*0.45*	*0.06*	*0.15*	*0.12*	*1.00*				

[a] Solution compositions listed in Table I.
[b] The largest peak area in a given chromatogram was assigned a value of 1 and other peaks were normalized accordingly.
[c] Calculation of this section of the table is described in more detail in the text. Normalization involved a 3-step procedure: (a) peak areas for a given chromatogram were ratioed to the area of Nor; (2) These values were divided by the corresponding ratio for the standard used in a given experiment; and (3) The 'normalized' values were divided by the mole ratio of the amino acid to Nor in the corresponding starting solution (Table I).
* Values in rows corresponding to standards are averages of standard analyses.

retrieved 95% of the volume of liquid initially loaded (Table III). Consequently, the yields determined for this sample have the highest likelihood of accuracy. Yields of both of the amino acids in Shot 64 were 40% of their initial concentrations, based on comparison with our MS calibration.

Interpretation of yields for Shot 77 was more problematic. The amount of liquid extracted from this capsule accounted for only 50% of the initial volume of liquid deposited. Yields for this experiment were greater than 100% for all of the amino acids except Phe. However, if we assume that the liquid was retained in the capsule prior to milling, and the difference in volume recovered can be accounted for by evaporative loss of H_2O, we obtain yields less than 100%, and the yields reported (Table IV) are lower bounds on the amount that survived.

Comparison of our yields for Shot 64 and our 'corrected' yields for Shot 77 reveal two points of interest. First, equivalent proportions of Lys and Nor, relative to one another, persisted in each shot. These two amino acids have yields very similar to those for Pro and Amb in Shot 77. Phe appears to be the most reactive of the five amino acids studied. The second point to note is that amino acids persisted to a greater extent in the capsule shocked to a higher pressure and temperature (see Table I). This is in agreement with the hypothesis (e.g., Blank and Miller, 1998) that pressure delays or inhibits breakdown due to thermal heating.

6.2.2. *Normalization of analyses*

By scaling our chromatography results so that the largest peak area is given a value of 1 and the other peak areas are scaled accordingly, we can compare the relative variations of amino acids within a given sample. Proportions of amino acids present in replicate analyses of a sample can be variable, reasons for which may be one or a combination of the following. Amino acids may be distributed heterogeneously within a sample vial as a consequence of density stratification, zwitterion clustering, or actual heterogeneity within a sample. Alternatively, the sample may have altered chemically over time, though they were stored in a low-temperature (4 °C) refrigerator prior to and between analyses. Finally, there may be some variation, probably on the order of a few percent, due to the manual selection of peak boundaries when determining relative areas corresponding to each amino acid's profile. We observed no systematic patterns in the variations, and this is an issue we will address in future efforts.

Typically, Nor exhibited the least variation ($\leq$15%) among replicate analyses, followed by Lys. Phe exhibited the greatest variation (>40%), consistent with the fact that it is the least stable and most volatile of the amino acids in water.

Although we were unable to recover measurable quantities of liquid from most of the capsules, we were able to extract a residue from inside the capsules using a water rinse. Analysis of this water subsequently revealed the presence of amino acids and other compounds. Details of the sampling procedure are discussed in the experimental section above. Usually, a capsule that appeared to have remained intact at the time of collection from the recovery chamber of the gun developed

one or more seepage points several hours to days following the experiment. We interpret this to be a consequence of the steel capsule's relaxation following deformation (e.g., bowing) during the shock experiment. Invisible microfractures in the steel could serve as conduits for sample fluid; these might expand as the capsule relaxed, resulting in the seepage. Because of the delay between sample recovery and sample analysis (typically on the order of weeks), the seepage usually evaporated and formed a brown dot-like stain 1–2 mm in diameter on the surface of a capsule. Alternatively, it adhered to the inside of the teflon sample container as a smaller, liquid bead. We collected this material, but we have no history of the volume fraction of initial solution it may represent, and therefore no dilution or evaporation history for quantitative determinations. We make the assumption that nonvolatile components (including the amino acids of our study) were retained in the brownish residue in proportions equivalent to those in the capsule prior to seepage; in this manner we are able to compare the relative variations among the amino acids and other compounds.

First, the areas beneath the mass chromatogram peaks corresponding to each amino acid were tabulated. These areas are proportional to the number of moles injected into the spectrometer. Since we do not have adequate control on the volume of shocked fluid recovered from each experiment, these inferred mole numbers cannot be represented as concentrations. The areas in a chromatogram are proportional to the product of the injected volume, the concentration of amino acids in the sample, and the dilution history of the sample. The relation between sample concentration and chromatogram area is described by the following,

$$(A_i)_n = s_i \times V \times d_n \times (c_i)_n \ ,$$

where $(A_i)_n$ is the area of the chromatogram peak corresponding to amino acid i in experiment n, s_i is a proportionality constant or the ratio of the chromatogram area to the numbers of moles injected into the instrument, V is the volume of solution injected, d_n is a dimensionless number representing the dilution history of the sample, and $(c_i)_n$ is the concentration of amino acid i in experiment n. The unknown in this expression is the dilution history of the sample, d_n. Comparisons between results from experiments whose dilution histories are unknown require normalization to eliminate this variable. We did this by selecting Nor as an arbitrary internal standard (but one whose concentration may have changed) and using the ratios of amino acid chromatogram areas to those of Nor.

$$(A_i/A_{NOR})_n = (s_i/s_{NOR}) \times (c_i/c_{NOR})_n \ .$$

Finally, we divided the 'normalized' ratio by the mole ratio of an amino acid to Nor present in the initial solution to eliminate the ratio (s_i/s_{NOR}):

$$(A_i/A_{NOR})_n/(A_i/A_{NOR})_{std} = (c_i/c_{NOR})_n/(c_i/c_{NOR})_{std} \ .$$

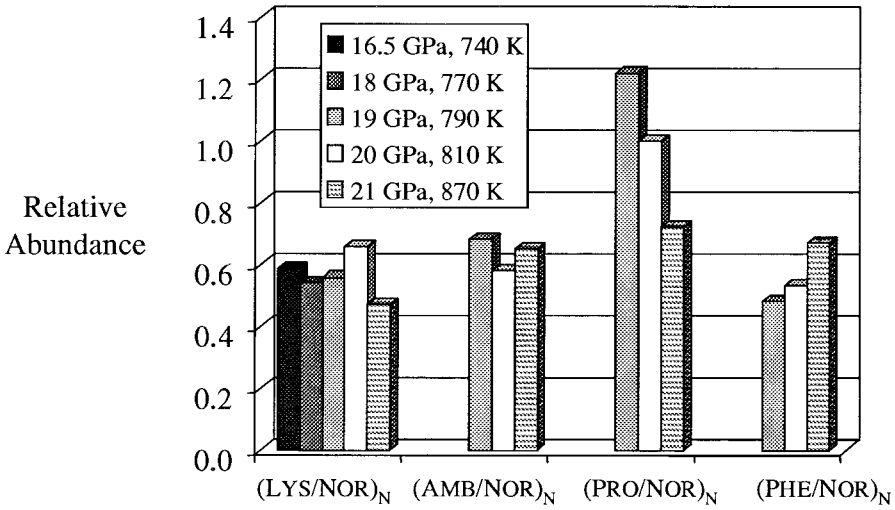

Figure 7. Variations in amino acid stabilities over a range of P,T conditions in samples that experienced the same duration of peak conditions (i.e., $\approx$1 μsec). Column patterns denote different experimental conditions; see legend. Note that an increase in P has a corresponding increase in T. Relative concentrations of four of the amino acids (Lys, Amb, Pro, Phe) are compared to that of Nor in the same experiment, and then normalized by making a ratio of the resulting value and a similarly determined value for the initial starting material to allow direct comparison among samples. (Details for determining the ordinate values are given in the text). Lys, Amb, and Phe exhibit lower stability ($\approx$45–65%) relative to Nor over the range of pressures investigated. At 19 GPa, Pro is more stable relative to Nor and has a relative abundance greater by nearly 20%. Pro becomes less stable relative to Nor with increasing pressure; its abundance is nearly equal to that of Nor at 20 GPa and by 21 GPa it has a relative value more akin to the other three amino acids. Phe exhibits the opposite trend with increasing pressure, becoming more stable relative to Nor from 19–21 GPa. The relative changes in abundance with increasing pressure for Lys and Amb show little variation over the range of our experiments. Values graphed are averages of the analyses reported in Table V.

The results are given in Table IV. We highlight several observations using histograms (Figures 7 and 8) to illustrate the changes in four of the amino acids (Lys, Amb, Pro, Phe) relative to Nor. For a given amino acid ratio, histogram columns are placed in order of increasing pressure in Figure 7, which shows the reactivity of the amino acids with increasing P,T. Relative to Nor, Lys and Amb do not change significantly as pressure increases. Pro decreases relative to Nor, while Phe increases with pressure relative to Nor.

6.2.3. *Kinetic Controls*

Samples in our study experienced peak conditions for periods of time differing by a factor of 2 (Table II). We can compare the influence of kinetics on the amino acid reactivities by considering 2 experiments that experienced the same P and T for different lengths of time. Shots 76 and 77 had peak conditions of 20 GPa and 810 K, yet the duration of these peak conditions was $\sim$2 $\times$ greater (0.95 vs. 1.7 μs) in

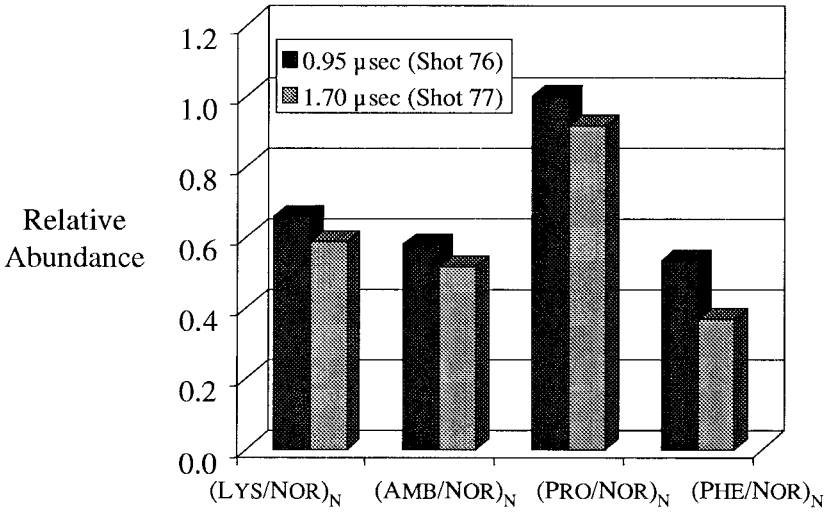

Figure 8. Influence of kinetic control on amino acid reactivity. Data of two samples that experienced similar peak conditions (20 GPa, 810 K) for shock pulses of duration different by a factor of ≈2. Normalization procedure described in the text. The four amino acids, Lys, Amb, Pro, Phe, decrease in abundance relative to Nor with increased shock pulse duration and thus have greater reactivity than Norvaline. Phe exhibits the greatest change between the two experiments, with a ≈30% decrease relative to Nor in the longer-pulse experiment; the other amino acids decrease by roughly 10% relative to Nor. Values graphed are averages of the analyses reported in Table V.

shot 77. The concentrations of all four amino acids (Lys, Amb, Pro, Phe) decrease relative to Nor when the peak conditions last longer (Figure 8). The differences vary, from 8–30%, with Amb showing the least change, and Phe showing the most. Phe appears to be the most reactive of the amino acids. Already, based on a factor of 2 variation in the shock pulse time, we observe evidence that kinetic effects have an important influence on the reactivity of our amino acids.

7. Reaction products

Analysis of the shocked samples revealed the presence of a number of new products, distinguishable through MS analysis. These products persist at levels several times to several orders of magnitude lower than the surviving amino acids. On the basis of mass to charge ratios (m/z), we interpret them to be dimers formed from the original amino acids. A representative chromatogram of a shocked sample (Figure 9a–c) shows a selection of peaks corresponding to these compounds for comparison with surviving amino acids.

We further interpret the structures of the dimers to correspond to di-peptides and cyclic peptides (diketopiperazines). A peptide bond forms via a dehydration synthesis reaction between the carboxy group of the first amino acid with the amino

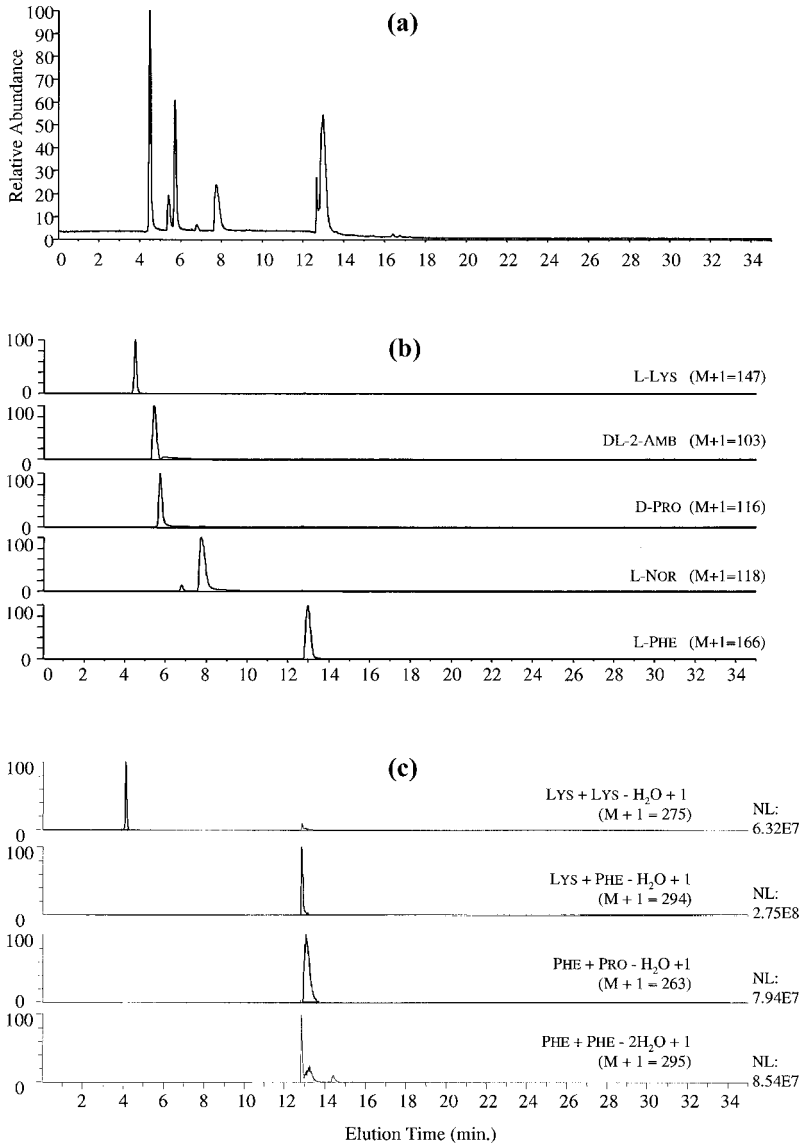

Figure 9. Representative (a) TIC and (b), (c) Selected Ion Chromatograms (SIC) measured for the sample from Shot 72, which contained 5 amino acids. (b) Note that the majority of the peak areas in the TIC are accounted for by the 5 amino acids. Other peaks identified correspond to higher m/z-value products – having the same mass as dimers and cyclic dimers formed from the five initial amino acids. (c) Assignments of peaks illustrated here have been confirmed by LCMS comparison with purchased dipeptide standards; see Table V for a summary listing. Relative scaling factors (indicated by 'NL') for the dimer products are denoted on the right side of the corresponding chromatogram (the larger scale factor indicates less relative abundance); the areas of the dimer compounds are substantially smaller than areas attributed to amino acids. Negligible quantities of products associated typically with pyrolysis were identified in our mass scans, though specific mass searches were performed.

group of the second amino acid. Two amino acids linked together by a peptide bond comprise a dipeptide (Equation (1)):

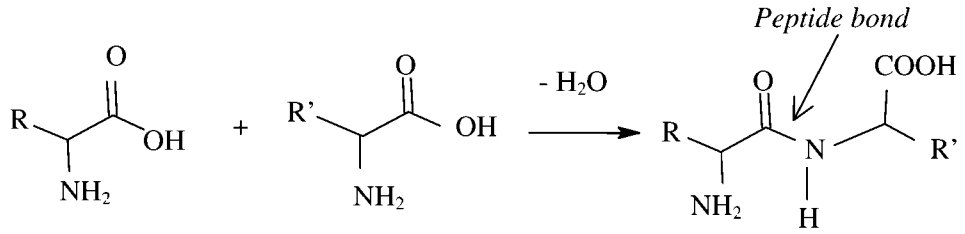

Equation (1).

When R and R′ are different, at least two isomers are possible. However, if R and R′ are the same, only one isomer is possible, unless the amino acid has more than one amino group. The presence of its two amine groups allows Lys to react with another amino acid to form at least 4 dimer isomers.

While it is possible to form anhydride with loss of H_2O resulting in a compound isomeric with the dipeptide (Equation (2)),

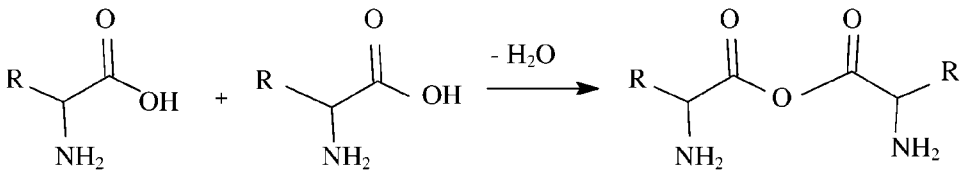

Equation (2).

these molecules will be susceptible to hydrolysis (Art Weber, personal communication; Stipanovic and Howell, 1982), and for this reason we deem them unlikely synthesis products. Anhydrides can initiate polymerization of the amino acids to form insoluble macromolecules (Greenstein and Winitz, 1961), though we have not detected such products to date.

A joining of two amino acids accompanied by loss of two water molecules yields a diketopiperazine (cyclic dimer) (Equation (3)).

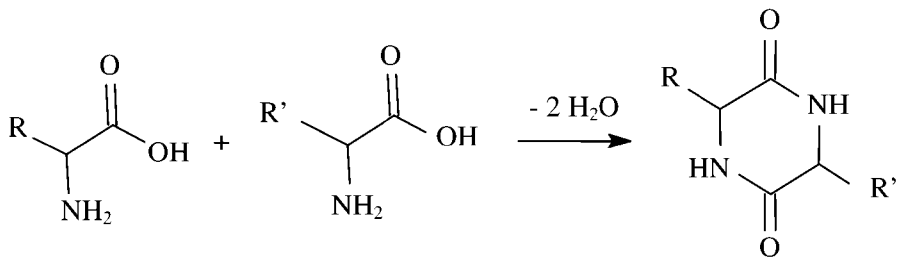

Equation (3).

TABLE V
Reaction product masses and identification

R	R′	Dipeptide		Cyclic dimer	
		M+1	Identified	M+1	Identified
Amb	Amb	189	X	171	–
Pro	Amb	201	X	183	X
Nor	Amb	203	X	185	–
Pro	Pro	213	X	195	X
Nor	Pro	215	X	197	X
Nor	Nor	217	X	199	X
Lys	Amb	232	–	214	–
Lys	Pro	244	–	226	–
Lys	Nor	246	X	228	–
Phe	Amb	251	X	233	X
Phe	Pro	263	X*	245	X
Phe	Nor	265	–	247	X
Lys	Lys	275	–*	257	–
Phe	Lys	294	X*	276	X
Phe	Phe	313	X	295	X*

Compounds were identified based on mass spectra. Mass peaks with elution times distinctive to those of the five amino acids are indicated by 'X'; '–' indicates a peak with the corresponding mass is present but not resolvable from individual amino acid peaks (and therefore mass spec determination is inconclusive as the dimer may have formed in the ion beam leading in to the mass spectrometer).
A '*' next to a mass number indicates that the dimer has been confirmed through comparison with a known dimer purchased from Aldrich Chemical Co.

The peak intensities for selected masses corresponding to cyclic dimer products are comparable in magnitude to the those of the linear dimers.

The masses of both linear and cyclic dimers possible from combinations of our initial amino acids are listed in Table V. Selected mass analysis of our chromatograms revealed peaks corresponding to all 30 of them, and most of the peaks had elution times distinctive from individual amino acids. Several cannot be confirmed, even tentatively, from their mass alone due to interference from the starting amino acids and the possibility that the dimers were formed during ionization and injection in to the mass spectrometer.

We have confirmed assignments for five dimers by comparison with dipeptides and a diketopiperazines purchased from Aldrich Chemical Co. (Figure 10). Confirmed products are indicated in Table V, and they correspond to the dimers shown

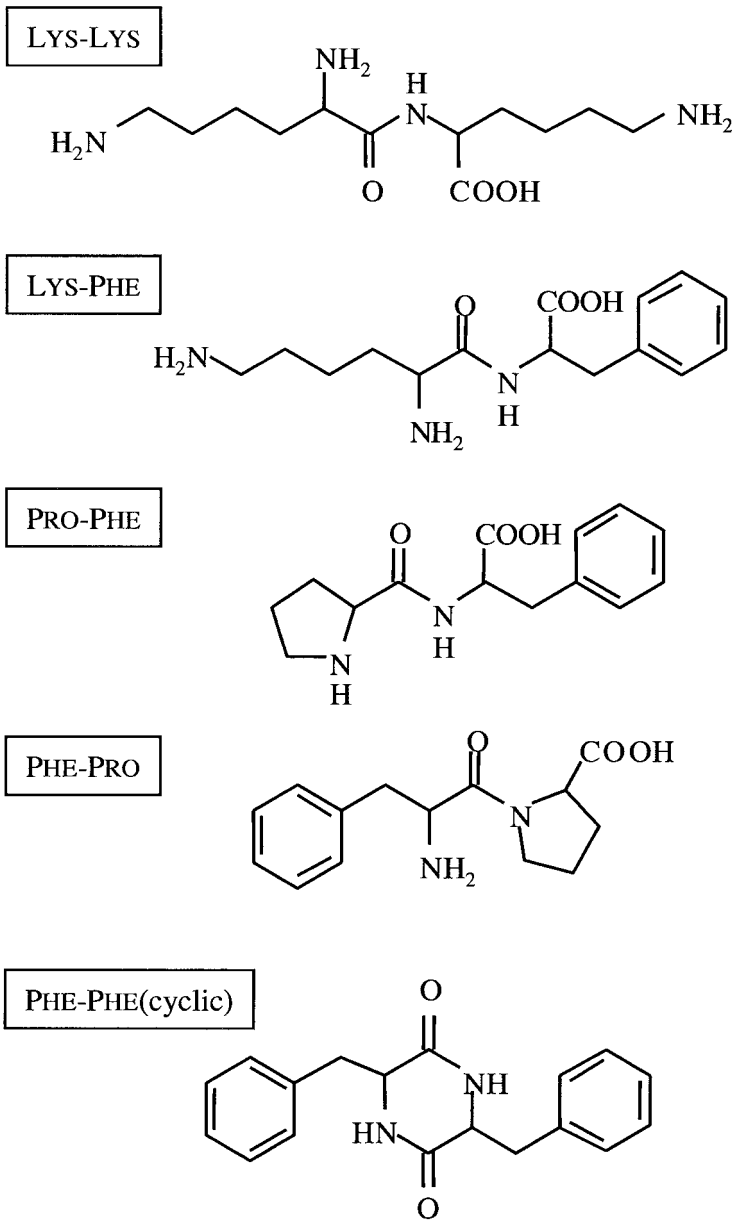

Figure 10. Amino acid dimers that have been identified in our samples and confirmed through comparison of elution times with those of known compounds purchased from Aldrich Chemical Co.

in Figure 9c. Through a calibration of the dimer, Lys-Lys, similar to that described earlier for the individual amino acids, we estimate that this dimer has an abundance on the order of 10% relative to Lys in several of the shocked samples. Semi-quantitative results (i.e, based on chromatogram peak intensity only) suggest that aromatic Phe is the most abundant. This is in keeping with the observation that Phe is the most reactive of the amino acids in our experiments. More than one peak with the same mass appears frequently in a chromatogram (see Figure 9) which we interpret to indicate the presence of isomers.

7.1. COMPARISON TO OTHER AMINO ACID CHEMISTRY

Pyrolysis of amino acids at ambient pressure and temperatures as high as 500 °C will cause their breakdown into constituent gases (CO_2, H_2O, NH_3, CO) and a variety of simple, volatile organic compounds (amines, nitriles, amides, hydrocarbons, etc.). In addition, amino acids may undergo simultaneously intermolecular condensation in to cyclic dipeptides in the yields of 5–20% (Ratcliff *et al*., 1974; Simmonds *et al*., 1972). Diketopiperazines can be hydrolyzed back to their component amino acids readily by short duration, rapid heating in the presence of water vapor (e.g., Basiuk and Douda, 1999).

In traditional thermolysis of amino acids, decarboxylation (Equation (4)) and deamination (Equation (5)) and are typical degradation pathways, occurring at fairly low temperatures (<350 °C):

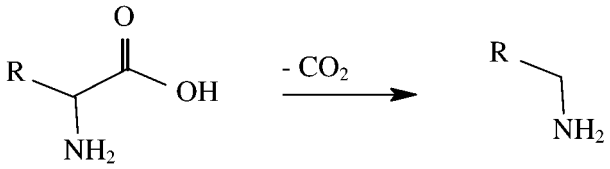

Equation (4).

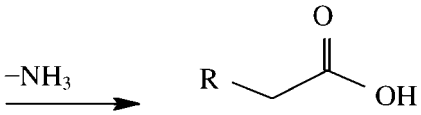

Equation (5).

Often, initial loss of the carboxyl group will be followed by loss of the amine group (cf., Rodante *et al*., 1992; 1997), though other pathways have been observed. For example, Bada and co-workers (1995) showed that alanine decomposes at an irreversible first-order rate to ethylamine at 240 °C, which decomposes at rate 40 times slower than alanine. Aspartic acid has been shown to undergo deamination to form ammonia and fumaric acid (Bada and Miller, 1970). In our analysis, we failed to detect measurable quantities of breakdown products. Fragmentation patterns of the

shocked amino acids were indistinguishable from those of the standard solutions. Volatile components in the samples would not be expected, given our method of sample extraction following a shock experiment.

Diketopiperazines have been reported as amino acid reaction products under a variety of conditions different from those occurring in our shock experiments. Gyore and Ecet (1975) noted that Phe forms its corresponding diketopiperazine at 195 °C, although upon further heating the product was completely degraded. Basiuk (1992) showed that several amino acids, including Nor, convert to the corresponding diketopiperazine by sublimation over silca at 220–240 °C. Further work by Basiuk and Douda (1999) revealed the preservation of aliphatic amino acids at the 1–10% level after exposure for short periods of time (≈10 min) to temperatures from 500–600 °C under N_2 or CO_2 atmospheres. Diketopiperazines were formed at typically 10% levels. Levels of both amino acids and cyclic dimers diminished as temperature increased.

The differences between the chemistry we observe and the chemistry observed in low pressure heating experiments may be understood qualitatively in terms of the well-known effect of pressure on organic reactions (albeit at lower pressure than those we employ). High pressure tends to reduce the reactive volume and activate the carboxylic acid group toward dehydration reactions leading to dimer formation. The activation volume $\Delta V^{\ddagger}$ is defined as the difference between the partial molar volume of the transition state and the initial states of the reactants in a chemical reaction (cf., Lowry and Richardson, 1987). Increased pressures will tend to accelerate reactions with a negative volume of activation. Negative activation volumes are associated with bond formation, concentration of charge, and ionization during the formation of a transition state. By contrast, bond cleavage, dispersal of charge, neutralization in the transition state, and diffusion control, lead to positive activation volumes. Reactions that are expected to speed up with increasing pressure include those in which the products reflect a reduction in the number of molecules, reactions which proceed through cyclic or dipolar transition states (e.g., the alkylation of tertiary amines), and reactions inhibited by steric hindrance. Hydrogen bond formation is expected to cause a volume contraction because of the decrease in atomic distance and suppression of thermal motions (e.g., Suzuki and Tsuchiya, 1975; Sawamura *et al*., 1986). Sometimes there is a critical pressure below which a reaction does not appear to take place (or to be accelerated). This may be due to a change of state, a change in mechanism, or both.

In a dipeptide, the terminal amine and carboxyl groups are situated so that they can interact to form a 6-membered ring diamide (cf., Greenstein and Winitz, 1961, pp. 782–804 and references therein). Intramolecular reactions to form 6-membered rings are frequently much faster than their intermolecular analogs (Streitweiser *et al*., 1992). Therefore, the relative abundance of the linear and cyclic dimers to one another may reflect the length of the shock impact. Such correlations may reveal new kinetic information about these reactions and will be the focus of future study.

8. Conclusions

To assess the reactivity of organic matter under conditions relevant to cometary impact, we have developed a set of laboratory shock wave and analytical chemistry techniques to determine the reaction products in shock-induced aqueous solutions containing organic compounds and to examine the kinetic behavior of the various reactions. Our experiments to date span a shock pressure/temperature range of ≈5–21 GPa and 412–870 K.

The most significant conclusion of our study is the determination that a significant fraction of amino acids survived in all experiments.

By comparing runs with similar pressure and temperature but different shock pulse duration, we have established that shock chemistry is controlled kinetically and resolvable by our method. Future experiments should allow us to determine reaction rate laws.

The relative reactivity of the individual amino acids changes with peak conditions. This is suggestive of either substantial nonlinearity in the reaction rate laws, or perhaps a change in the dominant reaction mechanism with changing pressure and temperature. We see evidence for P-dominated reactions (e.g., dehydration and dimer formation.).

Recent numerical modeling (Blank and Miller, 1998; Pierazzo and Chyba, 1999) has led to the prediction that lower temperatures may occur in cometary impacts that previously supposed. This, together with the chemical inference that pressure may mitigate the extent of thermally-driven breakdown reaction, supports the argument that an extraterrestrial origin of life's building blocks is possible. Most previous numerical models have required the comet to impact an ocean in order to survive. Our recent numerical model (Blank and Miller, 1998) suggests that these exogenous compounds could also be concentrated in a terrestrial environment, in higher concentrations, where subsequent chemical evolution would be more likely. Regardless of its delivery point, the potential flux of organic matter to the earth by comet, recently considered to be inconsequential, may be significant.

The shock chemistry we are exploring is also relevant to the formation of comets themselves by impact aggregation of presolar materials, as well as the formation of other icy bodies in the solar system (e.g., Europa). Additionally, numerical models of impact scenarios, and our experimental results, may apply to cometary delivery of organic material planets, including Mars.

Acknowledgements

Discussions with Sherwood Chang have led to improvements in the focus and scope of this work. George T. (Rusty) Gray III of Los Alamos National Laboratory provided expert advice throughout the development of the liquid-recovery shock procedures. Sutacha Hongresawat (U. Chicago) assisted with several of the shock

experiments. Useful comments from three anonymous reviewers helped to improve the manuscript. JB thanks Hal Helgeson for hospitality at Prediction North. This work was supported by the National Science Foundation POWRE program (EAR-9753175) and the NASA Exobiology Program (NAG5-9260). Computational work was supported by the ASCI/Alliances Center for Astrophysical Thermonuclear Flashes at the University of Chicago (DOE contract B341495). The effort at Argonne was performed under the auspices of the Office of Basic Energy Sciences, Division of Chemical Sciences, U.S. Department of Energy (contract W-31-109-ENG-38).

References

Ahrens, T. J., Blank, J. G., Hunt, J. E. and Winans, R. E.: 2001, Reversed-Phase High Performance Liquid Chromatography/Atmospheric-Pressure Chemical Ionization-Mass Spectrometry Method for Analyzing Free Amino Acids, submitted to *J. Chromatography*.

Asano, T. and LeNoble, W. J.: 1978, Activation and Reaction Volumes in Solution, *Chemical Reviews* **78**, 407–489.

Bada, J. L. and Miller, S. L.: 1970, Kinetics and Mechanism of the Reversible Nonenzymic Deamination of Aspartic Acid, *Journal of the American Chemical Society* **92**, 2774–2782.

Bada, J. L., Miller, S. L. and Zhao, M.: 1995, The Stability of Amino Acids at Submarine Hydrothermal Vent Temperatures, *Origins of Life and Evolution of the Biosphere* **25**, 111–118.

Barak, I. and Bar-Nun, A.: 1975, The Mechanisms of Amino Acid Synthesis by High Temperature Shock-Waves, *Origins of Life and Evolution of the Biosphere* **6**, 483–506.

Basiuk, V. A.: 1992, Condensation of Vaporous Amino Acids in the Presence of Silica. Formation of Bi- and Tricyclic Amidines, *Origins of Life and Evolution of the Biosphere* **22**, 333–348.

Basiuk, V. A. and Douda, J.: 1999, Pyrolysis of Simple Amino Acids and Nucleobases: Survivability Limits and Implications for Extraterrestrial Delivery, *Planetary and Space Science* **47**, 577–584.

Blank, J. G., Cody, G. D., Hazen, R. M., Hemley, R. J., Mao, H.-K., Struzhkin, V. V. and Yoder Jr., H. S.: 1997, In-situ Monitoring of the Stability of Organic Compounds in Aqueous Solutions at High Pressure and Temperature, *Eos* **78**, 327.

Blank, J. G. and Miller, G. H.: 1998, 'The Fate of Organic Compounds in Cometary Impacts', in A. F. P. Houwing, A. Paull, R. R. Boyce, P. M. Danehy, M. Hannemann, J. J. Kurtz, T. J. McIntyre, S. J. McMahon, D. J. Mee, R. J. Sandeman and H. Tanno (eds.), *Proceedings of the 21st International Symposium on Shock Waves*, Panther Press, Fyshwick, Australia, pp. 1467–1472.

Chyba, C. F. and Sagan, C.: 1992, Endogenous Production, Exogenous Delivery and Impact-Shock Synthesis of Organic Molecules: An Inventory for the Origins of Life, *Nature* **355**, 125–132.

Chyba, C. F. and Sagan, C.: 1997, 'Comets as a Source of Prebiotic Organic Molecules for the Early Earth', in P. J. Thomas, C. F. Chyba and C. P. McKay (eds.), *Comets and the Origin and Evolution of Life*, Springer, New York, pp. 147–173.

Chyba, C. F., Thomas, P. J., Brookshaw, L. and Sagan, C.: 1990, Cometary Delivery of Organic Molecules to the Early Earth, *Science* **249**, 366–373.

Clark, B. C.: 1987, Comets, Volcanism, the Salt-Rich Regolith, and Cycling of Volatiles on Mars, *Icarus* **71**, 250–256.

Clark, B. C.: 1988, Primeval Procreative Comet Pond, *Origins of Life and Evolution of the Biosphere* **18**, 209–238.

Cronin, J. R. and Chang, S.: 1993, 'Organic Matter in Meteorites: Molecular and Isotopic Analyses of the Murchison Meteorite', in J. M. Greenberg, C. X. Mendoza-Gómez and V. Pirronello (eds.),

The Chemistry of Life's Origins, Kluwer Academic Publishers, Dordrecht, The Netherlands, pp. 209–258.

Cronin, J. R. and Pizzarello, S.: 1986, Amino Acids of the Murchison Meteorite III: Seven Carbon Acyclic Primary A-Amino Alkanoic Acids, *Geochimica et Cosmochimica Acta* **50**, 2419–2427.

Davidson, D. F., DiRosa, M. D., Hanson, R. K. and Bowman, C. T.: 1993, A Study of Ethane Decomposition in a Shock Tube Using Laser Absorption of CH_3, *International Journal of Chemical Kinetics* **25**, 969–982.

Davis, L. L. and Brower, K. R.: 1996, Reactions of Organic Compounds in Explosive-Driven Shock Waves, *Journal of Physical Chemistry* **100**, 18775–18783.

Decarli, P. S. and Meyers, M. A.: 1981, 'Design of Uniaxial Strain Shock Recovery Experiments', in M. A. Meyers (ed.), *Shock Waves and High Strain Rate Phenomena in Metals*, Plenum, New York, 341 p.

Degens, E. T. and Bajor, M.: 1962, Amino acids and sugars in the Brudesheim and Murray Meteorites, *Naturwissenschaft* **49**, 605–606.

Dodson, B. W. and Graham, R. A.: 1982, 'Shock-Induced Organic Chemistry', in W. J. Nellis, L. Seaman and R. A. Graham (eds.), *Shock Waves in Condensed Matter*, American Institute of Physics/Springer-Verlag, New York, pp. 42–51.

Dremin, A. N. and Babare, L. V.: 1982, 'The Shock Wave Chemistry of Organic Substances', in W. J. Nellis, L. Seaman and R. A. Graham (eds.), *Shock Waves in Condensed Matter*, American Institute of Physics/Springer-Verlag, New York, pp. 27–41.

Fomenkova, M. N., Chang, S. and Mukhin, L. M.: 1994, Carbonaceous Components in the Comet Halley Dust, *Geochimica et Cosmochimica Acta* **58**, 4503–4512.

Gibbons, R. V. and Ahrens, T. J.: 1971, Shock Metamorphism of Silicate Glasses, *Journal of Geophysical Research* **76**, 5489–5498.

Gray III, G. T.: 1993, 'Influence of Shock-Wave Deformation on the Structure/Property Behavior of Materials', in J. R. Asay and M. Shahinpoor (eds.), *High-Pressure Shock Compression of Solids*, Springer-Verlag, New York, pp. 187–215.

Greenberg, J. M.: 1993, 'Physical and Chemical Composition of Comets – From Interstellar Space to Earth', in J. M. Greenberg, C. X. Mendoza-Gómez and V. Pirronello (eds.), *The Chemistry of Life's Origins*, Kluwer Academic Press, Dordrecht, The Netherlands, pp. 195–207.

Greenstein, J. P. and Winitz, M.: 1961, *The Chemistry of the Amino Acids*, Vol. I–III, Wiley & Sons, N.Y., 2872 p.

Gyore, J. and Ecet, M.: 1975, 'Thermal Behavior of Phenylalanine and Aminophenylalanine', in I. Buzas (ed.), *Proceedings of the 4th International Conference on Thermal Analysis*, Vol. 2, Heyden Press, London, England, pp. 387–394.

Hidaka, Y., Taniguchi, T., Kamesawa, T., Masaoka, H., Inami, K. and Kawano, H.: 1993, High Temperature Pyrolysis of Formaldehyde in Shock Waves, *International Journal of Chemical Kinetics* **25**, 305–322.

Hills, J. G. and Goda, M. P.: 1993, The Fragmentation of Small Asteroids in the Atmosphere, *Astronomical Journal* **105**, 1114–1144.

Huebner, W. F. and Boice, D. C.: 1992, Comets as a Possible Source of Prebiotic Molecules, *Origins of Life and Evolution of the Biosphere* **21**, 299–315.

Irvine, W. M., Dickens, J. E., Lovell, A, J., Schloerb, F. P., Senay, M., Bergin, E. A., Jewitt, D. and Matthews, H. E.: 1998, Chemistry in Cometary Comae, *Faraday Discussions* **109**, 475-492.

Kieffer, S. W.: 1971, Shock Metamorphism of the Coconino Sandsotone at Meteor Crater, Arizona, *Journal of Geophysical Research* **76**, 5449–5473.

Kissel, J., Brownlee, D. E., Büchler, K., Clark, B. C., Fechtig, H., Grün, E., Hornung, K., Igenbergs, E. B., Jessberger, E. K., Krueger, F. R., Kuczera, H., McDonnell, J. A. M., Morfill, G. M., Rahe, J., Schwehm, G. H., Sekanina, Z., Utterback, N. G., Völk, H. J. and Zook, H. A.: 1986, Composition of Comet Halley Dust Particles from Giotto Observations, *Nature* **321**, 336–337.

Kissel, J. and Krueger, F. R.: 1987, The Organic Component in Dust from Comet Halley as Measured by the PUMA Mass Spectrometer on Board Vega 1, *Nature* **326**, 755–760.

Kvenvolden, K., Lawless, J., Pering, K., Peterson, E., Flores, J., Ponnamperuma, C., Kaplan, I. R. and Moore, C.: 1970, Evidence for Extraterrestrial Amino-Acids and Hydrocarbons in the Murchison Meteorite, *Nature* **228**, 923–926.

Lerner, N. R., Peterson, E. and Chang, S.: 1993, The Strecker Synthesis as a Source of Amino Acids in Carbonaceous Chondrites: Deuterium Retention During Synthesis, *Geochimica et Cosmochimica Acta* **57**, 4713–4723.

Lowry, T. H. and Richardson, K. S.: 1987, *Mechanism and Theory in Organic Chemistry*, 3rd ed., Harper Collins Publishers, New York, 1090 p.

Mackie, J. C., Colket III, M. B. and Nelson, P. F.: 1990, Shock Tube Pyrolysis of Pyridine, *Journal of Physical Chemistry* **94**, 4099–4106.

Marsh, S. P.: 1980, *LASL Shock Hugoniot Data*, University of California Press, Berkeley, 327 p.

Matsumoto, K. and Acheson, R. M.: 1991, *Organic Synthesis at High Pressures*, John Wiley & Sons, Inc., New York, 456 p.

McKay, C. P. and Borucki, W. J.: 1997, Organic Synthesis in Experimental Impact Shocks, *Science* **276**, 390–392.

Mertens, J. D., Chang, A. Y., Hanson, R. K. and Bowman, C. T.: 1989, Reaction Kinetics of NH in the Shock Tube Pyrolysis of HNCO, *International Journal of Chemical Kinetics* **21**, 1049–1067.

Miller, G. H.: 1997, Conditions for Single and Multimaterial Jets, *Proceedings of the 28th Lunar and Planetary Science Conference* **28**, 957–958.

Miller, G. H.: 1998, Jetting in Oblique, Asymmetric Impacts, *Icarus* **134**, 163–175.

Miller, G. H. and Puckett, E. G.: 1996, A High-Order Godunov Method for Multiple Condensed Phases, *Journal of Computational Physics* **128**, 134–164.

Miller, S. L. and Urey, H. C.: 1959, Organic Compound Synthesis on the Primitive Earth, *Science* **130**, 245–251.

Orava, R. N. and Whittman, R. H.: 1971, 'Techniques for the Control and Application of Explosive Shock Waves', in *Proceedings of the 5th International Conference on High Energy Fabrication*, University of Denver Press, Denver, p. 1–27.

Oró, J.: 1961, Comets and the Formation of Biochemical Compounds on the Primitive Earth, *Nature* **190**, 389–390.

Peterson, E., Horz, F. and Chang, S.: 1997, Modification of Amino Acids at Shock Pressures of 3 to 30 GPa, *Geochimica et Cosmochimica Acta* **61**, 3937–3950.

Pierazzo, E. and Chyba, C. F.: 1999, Amino Acid Survival in Large Cometary Impacts, *Meteoritics and Planetary Science* **34**, 909–918.

Ratcliff, M. A., Medley, E. E. and Simmonds, P. G.: 1974, Pyrolysis of Amino Acids: Mechanistic Considerations, *Journal of Organic Chemistry* **39**, 1481–1490.

Rodante, F., Fantauzzi, F. and Catalani, G.: 1997, Thermodynamics of Dipeptides in Water. V. Calorimetric Determination of Enthalpy Change Values Related to Proton Transfer Processes of a Series of Dipeptides in Water, *Thermochimica Acta* **296**, 15–22.

Rodante, F., Marrosu, G. and Catalani, G.: 1992, Thermal Analysis of Some α-Amino Acids with Similar Structures, *Thermochimica Acta* **194**, 197–213.

Russell, M. J., Hall, A. J., Cairns-Smith, A. G. and Braterman, P. S.: 1988, Submarine Hot Springs and the Origin of Life, *Nature* **336**, 117–121.

Sawamura, S., Tsuchiya, M., Taniguchi, Y. and Suzuki, K.: 1986, Effect of Pressure on the Dimerization of Benzoic Acid in n-Heptane, *Spectrochimica Acta* **42A**, 669–772.

Shock, E. L.: 1990, Geochemical Constraints on the Origin of Organic Compounds in Hydrothermal Systems, *Origins of Life and Evolution of the Biosphere* **20**, 331–367.

Shoemaker, E. M.: 1962, 'Interpretation of Lunar Craters', in Kopal, Z. (ed.) *Physics and Astronomy of the Moon*, Academic Press, New York, pp. 283–359.

Simmonds, P. G., Medley, E. E., Ratcliff, M. A. and Shulman, G. P.: 1972, Thermal Decomposition of Aliphatic Monoamino-Monocarboxylic Acids, *Analytical Chemistry* **44**, 2060–2066.

Snyder, D. E.: 1997, The Search for Interstellar Glycine, *Origins of Life and Evolution of the Biosphere* **27**, 115–133.

Steel, D.: 1992, Cometary Supply of Terrestrial Organics: Lessons from the K/T and the Present Epoch, *Origins of Life and Evolution of the Biosphere* **21**, 339–357.

Stipanovic, R. D. and Howell, C. R.: 1982, The Structure of Gliovirin, a New Antibiotic from Gliocladium Virens, *Journal of Antibiotics* **35**, 1326–1330.

Streitwieser, A., Heathcock, C. H. and Kosower, E. M.: 1992, *Introduction to Organic Chemistry*, 4th ed., Prentice Hall, New Jersey, 1256 p.

Suzuki, K. and Tsuchiya, M.: 1975, Effect of Hydrostatic Pressure on the Hydrogen Bond Formation Between Phenol and Dioxane in Hexane, *Bulletin of the Chemical Society of Japan* **48**, 1701–1704.

Thomas, P. J. and Brookshaw, L.: 1997, 'Numerical Models of Comet and Asteroid Impacts', in P. J. Thomas, C. F. Chyba and C. P. McKay (eds.), *Comets and the Origin and Evolution of Life*, Springer, New York, pp. 131–145.

Tingle, T. N., Tyburczy, J. A., Ahrens, T. J. and Becker, C. H.: 1992, The Fate of Organic Matter During Planetary Accretion: Preliminary Studies of the Organic Chemistry of Experimentally Shocked Murchison Meteorite, *Origins of Life and Evolution of the Biosphere* **21**, 385–397.

Wu, C. H., Singh, H. J. and Kern, R. D.: 1987, Pyrolysis of Acetylene Behind Reflected Shock Waves, *International Journal of Chemical Kinetics* **19**, 975–996.

Zahnle, K. J. and Sleep, N. H.: 1997, 'Impacts and the Early Evolution of Life', in P. J. Thomas, C. F. Chyba and C. P. McKay (eds.), *Comets and the Origin and Evolution of Life*, Springer, New York, pp. 175–208.